ATTACHMENT 1

COAST & HARBOR ENGINEERING

Technical Memorandum 5

JETWASH Model Boundary Layer Development Analysis

A boundary layer is the zone of flow in the immediate vicinity of the bottom surface in which the motion of the fluid is affected by the frictional resistance exerted by the bottom. Schematically, the boundary layer for propwash flow is shown in Figure 1.

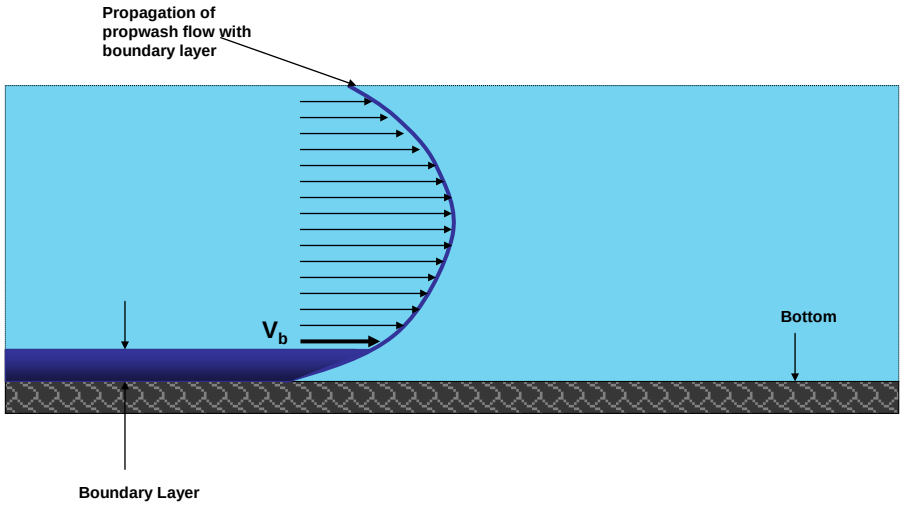

Figure 1. Schematic of propagation of propwash flow with boundary layer

For still water (when flow velocity equals zero) the boundary layer does not exist. The boundary layer forms as a consequence of the boundary's frictional resistance applied to the flowing fluid.

Theoretically, it should take some period of time to form a fully developed boundary layer after flow suddenly starts in still water (for example, a boat producing propwash moves over the lake). If it were possible to measure propwash velocity during boundary layer development, it is likely that this velocity would be larger than the velocity at the same elevation in the case with fully developed the boundary layer. Figure 2 shows schematically the theoretical differences in propwash velocities for flows with and without a boundary layer.

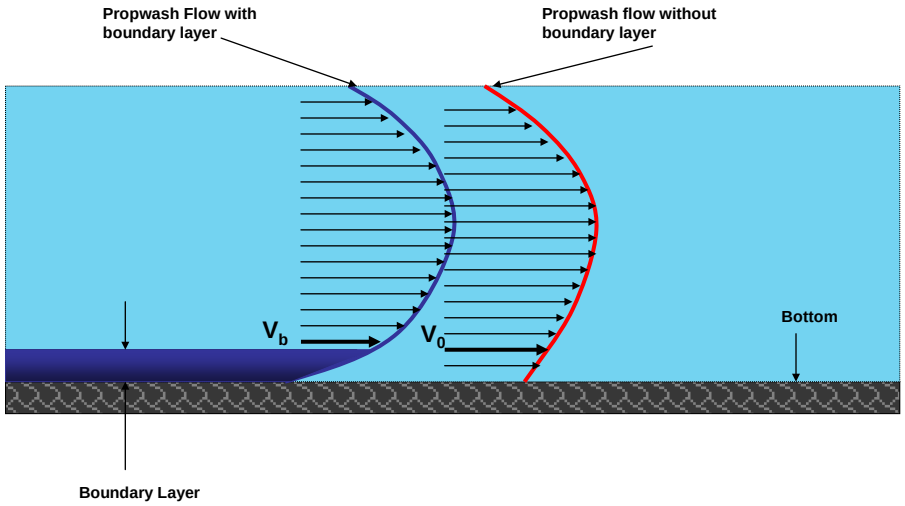

Figure 2. Propagation of propwash flow with and without a boundary layer

The JEWASH model does not account directly for existence of a boundary layer. It does; however, include other conservative factors that indirectly account for the boundary layer. Therefore, there has been concern that actual propwash flow with a non-established boundary layer (initial impingement of the jet at the bottom) may affect bottom sediment (cap material) with larger shear stress than that calculated with velocities predicted by JETWASH at specified heights above the bottom.

At present, no methods exist for assessing boundary layer development for conditions such as propeller wash impinging on the sediment bed. Shear stress in the non-fully developed boundary layer is a fundamental theoretical problem that cannot be solved in the scope of current study. However, it can be demonstrated that JETWASH results are sufficiently conservative to compensate for boundary layer development effects. To do this, Coast & Harbor Engineering (CHE) assumed that shear stress at the bottom is proportional to bottom flow velocity at a small distance above the bed. JETWASH velocity results calculated for cases near a bottom boundary and with no bottom boundary were compared. It can be reasonably assumed that near-bottom velocities during boundary layer development will not be greater than those from the no bottom boundary case. The goal of the following discussion is to 1) demonstrate that JETWASH conditions with a boundary produce higher velocities at water depths near the boundary than the no-boundary conditions. From this, it can then be demonstrated that 2) bottom shear stress is greater in JETWASH than for the comparable estimates for the period during boundary layer development due to the built-in conservatism in JETWASH. A height above the sediment bed of 15 cm was selected as the height at which velocities were compared, and is defined herein as the "near-bottom" velocity from which bottom shear stress is calculated. This height is sufficiently close to the bottom so that shear stress estimates will be conservative, both under developing and developed boundary layer conditions.

Denoting instantaneous actual bottom propwash velocity without a boundary layer (infinite water depth) as V_0 and JETWASH predicted velocity at the same elevation as Vj, the evaluation can be summarized as follows:

- If $V_0 > V_j$, then JETWASH may not be conservative enough and additional analysis of sediment stability is required.
- If $V_0 < V_j$, JETWASH is conservative enough and can be used for the design of cap layer.

The objective of the analysis is to determine the difference between propwash velocity at the bottom with a not fully-developed boundary layer and propwash velocity (of the same source) predicted by the JETWASH model.

No reliable and commonly accepted methods (formulae, models) exist to compute flow velocity for developing boundary layer conditions during jet impingement. Therefore, the above described JETWASH comparison tests were applied. The test includes computing near-bottom velocity with JETWASH at the existing water depth (boundary layer included), and at the same elevation but with the bottom moved to infinite depth. Figure 3 schematically shows the infinite depth concept for this evaluation.

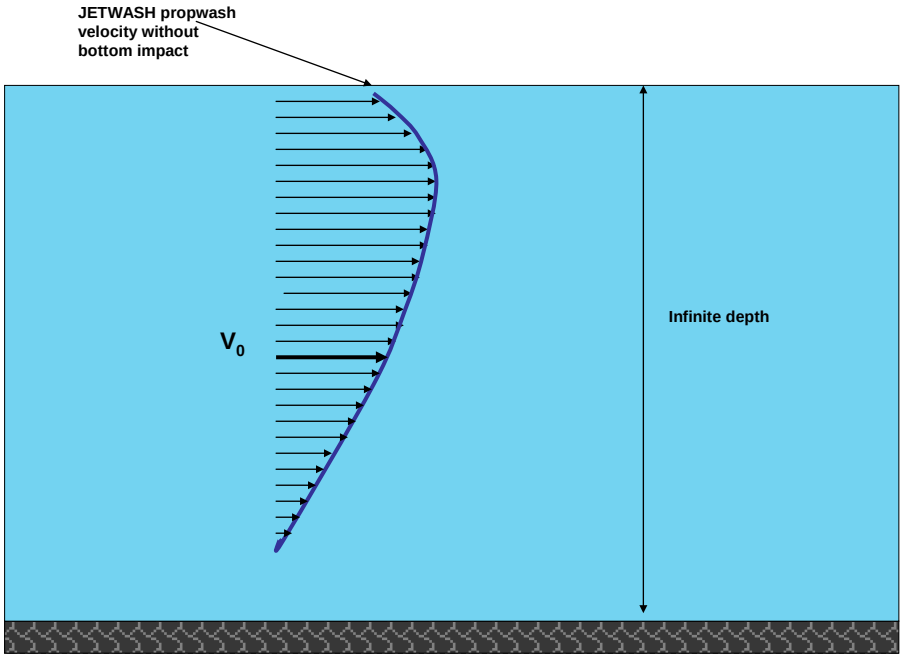

Figure 3. Schematic of computational test, flow velocity at a fixed elevation with bottom moved to infinite depth

A standard definition for a bottom boundary layer is: "…zone of flow in the immediate[1] vicinity of bottom surface in which the motion of the fluid is affected by the frictional resistance exerted by the bottom" (Middleton and Southard 1984). Therefore, velocity V_0 is not affected by frictional resistance of the bottom, and we can assume V_0 is equal

[1] For certain conditions it may influence much of the water column

to or greater than the near-bed velocity in developing boundary layer conditions. This evaluation includes computing bottom velocity with JETWASH for various conditions (including a Fox River example that is used in Technical Memo 3) and repeating the computations for cases with the bottom at such depth that it does not affect the flow. JETWASH algorithms are designed such that the propeller-induced total flux for each case (depth-limited and infinite depth) is equal (assuming identical prop conditions). Therefore, JETWASH forces the depth-limited case to include increased near-bottom velocities to compensate for areas in the infinite depth case that are below the natural water depth in the depth-limited case but where flux still occurs (i.e., JETWASH reflects the additional flux back up into the near-bottom layer of the depth-limited case; thus, the built in near-bottom conservatism). The results of a sample computation are presented in Table 1. Figure 1 is an example of velocity profile computations at 5.9 ft behind the prop showing velocities at heights of 5 to 30 cm above the bottom for 5-ft water depth conditions. The built-in conservatism of JETWASH can be seen in the depth-limited profile, which does not fit the 'typical' near-bottom velocity profile where there is a rapid decrease near-bottom. This is due to the reflection of the infinite-depth case velocities back into the boundary layer.

Table 1, Results of JETWASH computational test

Monterey, 5-ft water depth	**Velocity at 15 cm above bottom (ft/sec)**	
Distance behind prop (ft)	**With bottom**	**No bottom effect**
4.8	5.907	5.907
5.9	11.489	9.549
7.1	13.205	10.600

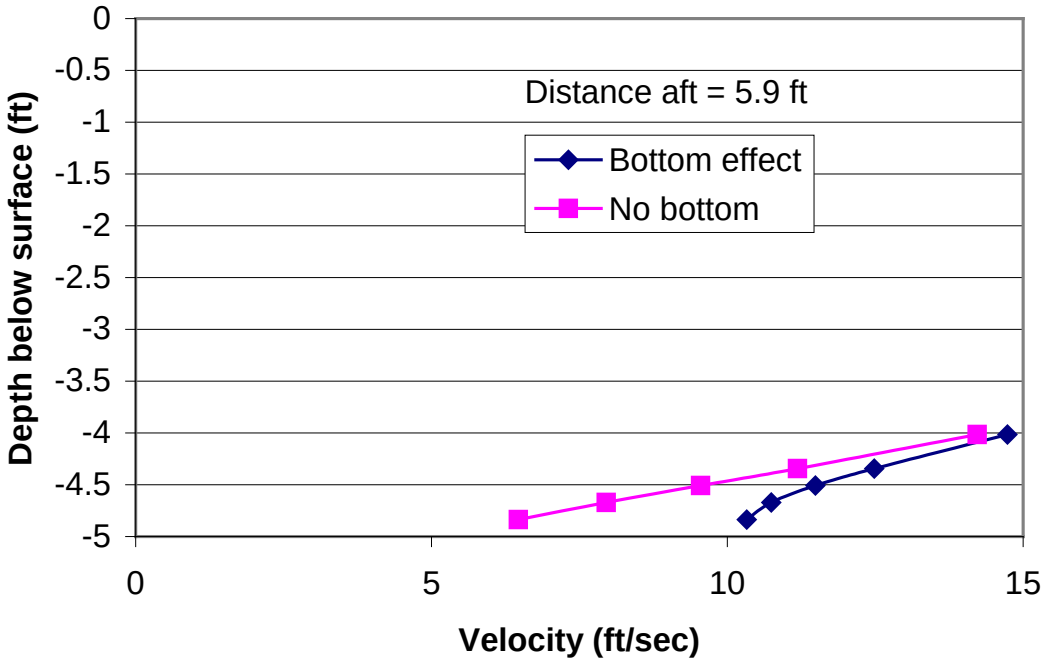

Figure 4. Example of JETWASH computational test, Monterey boat in 5-ft depth

Based on the computational test, it is concluded that because the JETWASH model incorporates enough conservative assumptions, the calculated bottom velocity is higher than that for the case of a non-developed boundary layer. Based on these computational tests and the JETWASH algorithms that inherently increase near-bottom velocities to account for flux balance, it can be concluded that the JETWASH assumptions will always provide conservative bottom shear stress during both developing and developed boundary layer calculations. Therefore, the JETWASH model is considered appropriately conservative for the Fox River propwash analysis without modifications.

REFERENCE

Middleton, Gerard V. and Southard, John B. 1984. Mechanics of Sediment Movement. S.E.P.M. Short Course No. 3, 2nd Edition. SEPM Tulsa, OK 74159-0756

ATTACHMENT 2

PROPWASH AND VESSEL HYDRODYNAMICS STUDY
EAST WATERWAY OPERABLE UNIT SRI/FS
SEDIMENT TRANSPORT EVALUATION

COAST & HARBOR
ENGINEERING

TABLE OF CONTENTS

FIGURES

TABLES

COAST & HARBOR ENGINEERING

Technical Report

Propwash and Vessel Hydrodynamics Study – East Waterway Operable Unit SRI/FS Sediment Transport Evaluation

1. Introduction

This Technical Report presents the modeling approach and results of propwash and pressure field analyses conducted by Coast & Harbor Engineering, Inc. (CHE) for the Port of Seattle, as part of the project team performing a SRI/FS for the East Waterway Operable Unit. Propwash modeling results are presented as near bottom velocities and bed shear stresses for each modeled scenario. The information and data from this technical report was the basis for Section 5, Propwash Modeling and Vessel Operations in the East Waterway of the Supplemental Remedial Investigation Feasibility Study Report, Sediment Transport Evaluation Report

Impact analysis from vessel hydrodynamics on bottom sediment was limited in this study to propwash and pressure field. The study purpose is to develop information for characterizing sediment transport dynamics in East Waterway. Figure 1 shows the study area location.

Figure 1. Location of East Waterway study area for vessel hydrodynamics

2. Propwash Modeling Methodology

2.1. Propwash Analysis Areas

The East Waterway was divided into areas in which activities and vessel types were similar. Fourteen separate areas and subareas were identified and provided by AnchorQEA. Figure 2 shows the areas in the waterway identified by number for developing analysis scenarios.

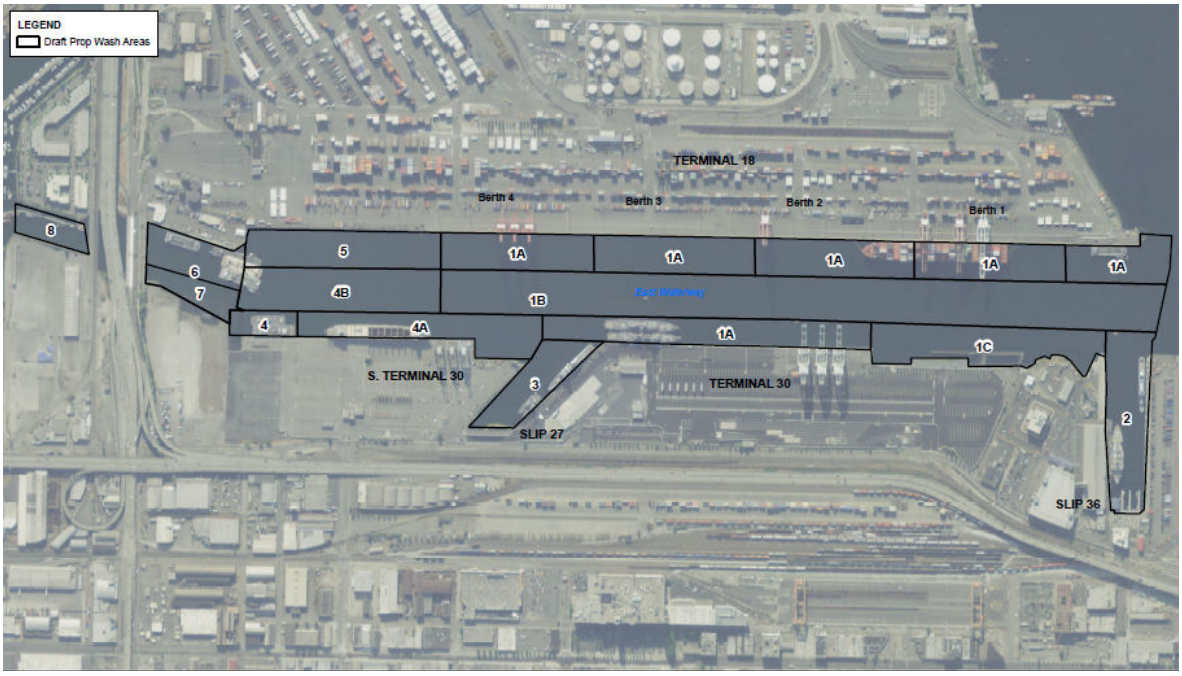

Figure 2. Study areas comprising the propwash modeling analysis of East Waterway (source: Anchor QEA)

The largest ships in the waterway are container carriers that call at the northern half of Terminal 18, on the west side of the waterway (Area 1a—see Figure 2). Berths are located at the terminal according to stationing from the northern end. Berths 1 and 2 handle the largest ships and extend from Station 500 to Station 2600 feet. Berths 3 and 4, which handle smaller container ships, extend from Station 2700 to Station 4800 feet and are also designated Area 1a. Ships approach these berths bow-first, under the assistance of at least two tugs. The ship's bow thruster is used to help steer the ship in the waterway. These vessels are turned in Elliott Bay, not in the waterway.

Farther south at Terminal 18 the pier is less used, and is the location where a 600-ft-long ship with one specific cargo calls approximately four times per year (Area 5). The ship is moved only under tug power.

The north end of the waterway on the east side is the location of Slip 36, where Coast Guard vessels dock (Area 2).

Container ships call at Terminal 30 (Area 1a), and are moved into the waterway stern-first using at least two tugs. The ship's bow thruster is used to help steer the ship within the waterway.

The part of Terminal 30 shown in Figure 2 as Area 1c is not used for berthing container ships, but the bottom sediment in Area 1c could be subjected to velocities generated by vessels transiting the waterway (Area 1b) or maneuvering while approaching a nearby berth.

Farther south, Slip 27 is the location where tugs and empty barges may be temporarily stored (Area 3).

The area southward of Slip 27 to the south end of the pier is now called South T30, but had an earlier designation of Terminal 25. The southern 400 feet (Area 4) is leased to Harley Marine Services (formerly Olympic Tug and Barge). Smaller container ships are expected to berth in the future between Areas 3 and 4 in an area designated Area 4a. Area 4b is affected by in-channel operations of vessels maneuvering at berths in Areas 4 and 5.

Southward from this area to the West Seattle Bridge, the west half of the channel is designated Area 6, and contains mooring facilities for oil barges and tugs owned by Harley Marine Services. The eastern half of this waterway is designated Area 7 and has no berths.

South of the bridge dominant use of Area 8 is for port facilities for Western Towboat tugs.

2.2. Propwash Numerical Models

Propwash modeling has been performed using two modeling systems: two-dimensional steady hydrodynamic model JETWASH, and three-dimensional (3-D) fully unsteady hydrodynamic model VH-PU. JETWASH modeling was conducted assuming that propeller (or any other source of propwash) and velocity field from this propeller is steady (no translation) relative to the bottom slope. Propwash simulations with VH-PU model have been conducted for conditions of propwash flow field moving with the propeller relative to the bottom surface at East Waterway[1].

[1] Results of simulation with VH-PU will be presented at the next phase of the study in relationship to depth of scour and sediment stability.

2.2.1. JETWASH

The modeling tool applied to determine near-bottom velocities, required for calculating bottom sediment transport and bottom shear stress, is the two-dimensional model JETWASH (CHE 2003). The JETWASH model simulates the velocity field created by propulsion systems and accounts for interaction of the velocity jet with the bottom boundary. The model and data requirements were summarized in a Technical Memorandum *Modeling Scenarios for East Waterway* (CHE 2011). The JETWASH model is based on a well-established and empirically verified theory of flow produced by a momentum jet. JETWASH has been tested and proven to be a reasonable engineering tool for propwash analysis. The JETWASH model has been accepted by EPA Region 8 and U.S. Army Corps of Engineers for analysis of sediment stability under impact from propwash of vessels ranging in size from small recreational boats to large ships. JETWASH also has been successfully applied for cases of ships equipped with thrusters.

The following describes the JETWASH model governing equations:

$$V_x = 2.78 * U_0 * \frac{D_0}{X} Exp(-15.43(\frac{z}{X})^2) + V_\alpha + V_\beta$$

Where:

U_0 = Jet velocity exiting propeller, computed with either of the following equations, depending on data availability:

$$U_0 = C_2 (P_d / D_p{}^2)^{1/3}$$

$$U_0 = 1.6 / D_p (T / p)^{1/2}$$

$$U_0 = 1.6 * n * D_p \sqrt{K_{tp}}$$

V_α = Additive velocities due to propeller shaft angle to the horizontal. It is always positive for angles between 0 and 180 degrees. V_α is a function of V_x (shaft parallel to the bottom) and angle of the shaft. Please note that V_α in the governing equation above is described conceptually. In computer code it is included in the first component of the equation[2].

V_β = Additive velocity due to bottom slope. It is equal to "0" for flat bottom (Fox River conditions).

[2] Based on propeller shaft angle, the radial distance from centerline to bottom is adjusted (reduced) which increases bottom velocity for positive angles.

Symbols in JETWASH and EMAP governing equations are identical and are described below:

V_x = Velocity at coordinate x and z

U_0 = Jet velocity exiting propeller

X = Horizontal distance from propeller

z = Radial distance from axis of propeller

D_p = Propeller diameter

$D_0 = 0.71 \cdot D_p$ for non-ducted propeller

P_d = Applied engine power

K_{tp} = Thrust coefficient

n = Propeller rps

T = Thrust

C_2 = Empirical coefficient

2.2.2. Unsteady Propwash Simulation

VH-PU is a 3-D curvilinear fully non-steady model that simulates velocities generated by ship propellers, including turbulence intensity and length scale in a given domain of arbitrary bottom and coastal topography. The VH-PU model was developed and tested with the support of a U.S. Civilian Research and Development Foundation grant.

VH-PU has been successfully used for various projects in the states of Washington, California, Texas, and Louisiana, and at overseas locations to determine propeller bottom scour and stability of under pier structures exposed to propeller wash effects from ferries, tug boats, and deep draft vessels. The VH-PU model accounts for the variable boundary layer conditions through the length scale of turbulent fluctuations in the boundary layer (equations 5 and 6 below) and friction velocity (equation 15 below).

The VH-PU model describes 3-D fields of velocities generated by ship propellers, including turbulence intensity and length scale in a given domain of arbitrary bottom topography. The model was developed on the basis of non-hydrostatic extension of the Princeton Ocean Model (POM) described by Blumberg and Mellor (1987).

2.2.3. Basic Equations

In the model the 3-D Reynolds averaged Navier-Stokes equations are used:

$$\frac{\partial u_i}{\partial xi} = 0, \qquad (1)$$

$$\frac{\partial u_i}{\partial t} + u_j \frac{\partial u_i}{\partial x_j} = -\frac{1}{\rho_0}\frac{\partial p}{\partial x_j} - \frac{\partial \overline{u_i u_j}}{\partial x_j} - g_j, \tag{2}$$

Where: $x_i = (x, y, z)$ are spatial coordinates, axis z is directed upward, $u_j = (u, v, w)$ are components of velocity, p is pressure, $g_j = (0, 0, g)$ is gravity, ρ_0 is constant density in Boussinesq approximation. The Reynolds stresses are modeled using the eddy viscosity approach:

$$\overline{u_i u_j} = -K_M \left(\frac{\partial u_i}{\partial x_j} + \frac{\partial u_j}{\partial x_i} \right) + \frac{1}{3} q^2 \delta_{ij}, \tag{3}$$

Where: eddy viscosity coefficient $K_M = S_M q\, l$ is related with kinetic energy of turbulence $\frac{1}{2} q^2 = \overline{u_i u_i}$ and length scale l. Here S_M is a model constant.

The model of turbulence is q-$q^2\, l$, which is a 3-D extension of the model of Mellor and Yamada (1982):

$$\frac{\partial q^2}{\partial t} + u_j \frac{\partial q^2}{\partial x_j} = -2\overline{u_i u_j}\frac{\partial u_j}{\partial x_j} + \frac{\partial}{\partial x_j} S_q q l \frac{\partial q^2}{\partial x_j} - 2\frac{q^3}{B_1 l}, \tag{4}$$

$$\frac{\partial q^2 l}{\partial t} + u_j \frac{\partial q^2 l}{\partial x_j} = -E_1 l \overline{u_i u_j}\frac{\partial u_j}{\partial x_j} + \frac{\partial}{\partial x_j} S_l l q \frac{\partial q^2}{\partial x_j} - \frac{q^3}{B_1}\left[1 + E_2 \left(\frac{1}{\kappa L} \right) \right], \tag{5}$$

In equation (5) the last term in square brackets is the wall function, which is necessary in a q-$q^2\, l$ model to correctly describe flow near the solid boundary. According to Mellor and Yamada (1982), the distance from a solid boundary L is:

$$L^{-1}(\mathbf{r}) = \frac{1}{2\pi} \iint \frac{dA(\mathbf{r}_0)}{[\mathbf{r} - \mathbf{r_0}]^3}, \tag{6}$$

Where: $\mathbf{r}$ is the radius vector for a given point, $\mathbf{r_0}$ is solid boundary. When the scale of computational domain is mainly a horizontal scale, then approximately:

$$L^{-1} = z^{-1} + (H - z)^{-1} \tag{7}$$

The constants of the turbulence model S_M, B_1, E_1, E_2 and S_l were determined by Mellor and Yamada (1982).

2.2.4. Boundary Conditions

The kinematic condition at the water surface z = $\eta(x,y,t)$ is:

$$\frac{\partial \eta}{\partial t} + u\frac{\partial \eta}{\partial x} + v\frac{\partial \eta}{\partial y} = w \tag{8}$$

The dynamic condition is:

$$k_m \frac{\partial \mathbf{V_h}}{\partial z} = \frac{\boldsymbol{\tau_0}}{\rho_o} \tag{9}$$

Where $\mathbf{V_h} = (u,v)$; $\boldsymbol{\tau} = (\tau^{(x)}, \tau^{(y)})$, is wind stress.

At the nearest computational layer $z = H + z_b$,

$$-u\frac{\partial H}{\partial x} - v\frac{\partial H}{\partial y} = w \tag{10}$$

and

$$k_m \frac{\partial \mathbf{V}_h}{\partial z} = \frac{\boldsymbol{\tau}_b}{\rho_o}, \tag{11}$$

Where:

$$\boldsymbol{\tau_b} = \rho_0 C_D \left|\mathbf{V_b}\right| \mathbf{V_b}, \tag{12}$$

$$C_D = \max\left(0.0025; \left(\frac{1}{\kappa}\ln(\frac{z_b + z_o}{z_o})\right)^{-2}\right) \tag{13}$$

The relevant boundary conditions for equations (4) - (5) at the surface and bottom are:

$$(q^2(\eta), q^2 l(\eta)) = (B_1^{2/3} u_\tau^2(0), 0) \tag{14}$$

$$(q^2(-H), q^2 l(-H)) = (B_1^{2/3} u_\tau^2(-H), 0),$$

$$(Q^2(-H), Q^2 l(-H)) = (B_1^{2/3} u_\tau^2(-H), 0) \tag{15}$$

Where $u_1(0)$ and $u_1(-H)$ are friction velocities.

The lateral conditions are given at the solid boundary and at the open boundary (see Figure 3). At the solid boundaries the non-slip conditions are used. At the open boundary a new boundary condition is used. It is based on a Newtonian relaxation technique for sea level. The computational domain is a closed area that is divided into an internal zone and relaxation zones along the open boundaries. The boundary conditions at the outer boundary of relaxation zones are non-slip conditions. The equation for surface elevation was derived by the integration of continuity equation (1) from bottom to surface. The modified equation is:

$$\frac{\partial \eta}{\partial t} + \frac{\partial \overline{u}(H+\eta)}{\partial x} + \frac{\partial \overline{v}(H+\eta)}{\partial y} = -\frac{\eta - \eta_B}{T}\alpha \tag{16}$$

The right hand side is a Newtonian relaxation term, where α is a relaxation parameter ($\alpha = 1$ in the relaxation zone and $\alpha = 0$ outside). η_b is prescribed elevation at the boundary and T is relaxation time, a parameter chosen to satisfy non-reflecting condition incoming in relaxation zone disturbances.

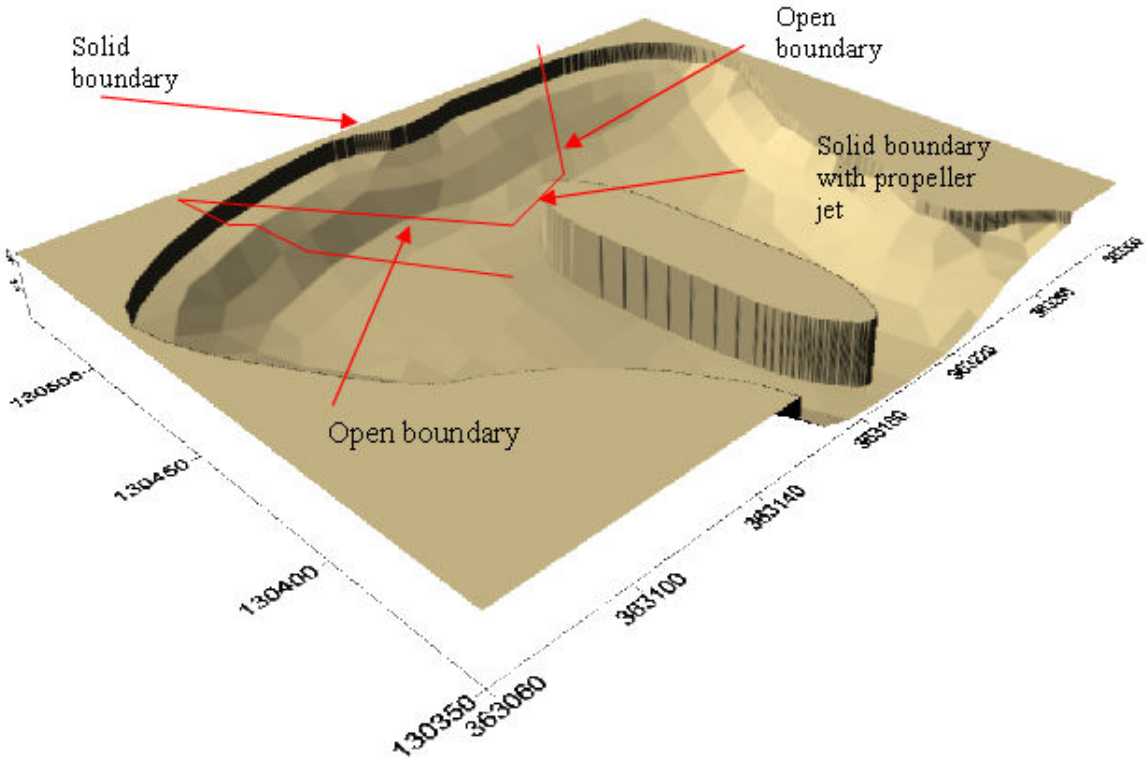

Figure 3. Scheme of computational area with different types of boundary

2.3. Shear Stresses Technical Approach

The approach to estimating the magnitude and location of bottom scour by ships' propulsion is to first simulate the flow velocity pattern created by the specific source installed on the ship, incorporating the channel depth at separate locations in the waterway. The second step is to apply the maximum bottom velocity in each location to determine the bottom shear stress.

The term near bottom velocity used in this report refers to velocity at 26 cm above bottom, which is applied in calculating critical shear stress of a bed surface particle. The height of 26 cm is arbitrary, but was the height of a velocimeter used in CHE field studies for validating the JETWASH model and has remained the reference height for calculating threshold of motion of bottom material. A logarithmic velocity profile is assumed to exist between the point of propwash velocity specification and the bottom (USACE, 2002). Shear stresses developed in the near-bottom propwash velocity field were calculated using the assumptions of rough, turbulent flow, logarithmic velocity profile, and the roughness factor k_s described below.

Bed shear stress τ_b developed by near bottom velocity is computed using modeled velocity U_{zref} at a specified height above the bottom, reference height z_{ref}, and assumes that a logarithmic velocity profile develops in the flow near the bottom. The velocity profile for dynamically rough flow over a granular boundary is

$$\frac{U_{zref}}{U_*} = 5.75 \cdot \log_{10}\left(\frac{Zref}{k_s}\right) + 8.5$$

Where,

U_{zref} is velocity at height $Zref$ above bottom

U_* is shear velocity = $\sqrt{\frac{\tau_b}{\rho}}$

$Zref$ is specified height above bottom (26 cm in this study)

κ_s is roughness length ($2 \cdot D_{90}$ in this study)

τ_b is bottom boundary shear stress = $\rho \cdot U_*^2$

Bottom roughness for use in calculating shear stress at the bottom of the East Waterway is assumed to be a function of sediment size. In the absence of bedforms, the roughness factor k_s has been variously defined by researchers as equal to the mean particle size or some other statistic. For example the original studies leading to the Karman-Prandtl logarithmic velocity profile equated k_s with the sediment diameter. Another example is a study by Gilliani *et al.* (2007) in which k_s was taken to be three times the D_{90} particle diameter for sediments having a D_{50} less than 0.05 mm. For consistency, the value of roughness for shear stress developed by bottom velocity due to propwash was defined as $2 \cdot D_{90}$ and adopted from bottom sediment characteristics presented by Anchor QEA in Section 6.2 of the main Sediment Transport Evaluation Report.

2.4. Test Matrix and List of Scenarios

Fifteen scenarios were developed for analyzing propwash effects. The scenarios consist of maneuvers of docking, undocking, and navigating the waterway; using ship's main power and thrusters; and using various types of tugs. Vessel types, maneuvers, area characteristics, and certain propwash parameters were specified for each area and were coordinated with the study team through a Technical Memorandum prepared by CHE (2011) and further developed in subsequent team discussions. Specifics of vessel types and propulsion were collected from public information of shipping lines, tug companies, and CHE archives. All simulations assumed the tide level was mean lower low water (MLLW). Simulations of all vessels, including tugs, in the docking and undocking maneuver assumed the source of propwash was stationary. Tugs transiting the waterway were assumed to make way at 4 knots. The total of 15 simulation scenarios and pertinent model input parameters are listed in Table 1.

Table 1. Modeling scenarios for East Waterway

Scenario Number	Propwash Area / Terminal	Depth at MLLW (ft)	Vessel Type / Name	Maneuver	Propulsion Type	Power Applied (kW)	Prop Speed (r.p.m.)	Prop Dia-meter (ft)	Depth Blw Prop Center (ft)
1	Area 1a, T 18 Berths 1 and 2	50	Container / Xin Mei Zhou	Docking	Ship's main power	6852	35	30.1	22
2	Area 1a, T 18 Berths 1 and 2	50	Container / Xin Mei Zhou	Undocking	Bow Thruster	3145	216	9.8	12.4
3	Areas 1a, 1b	50	Tractor Tug / Garth Foss	Docking a container ship	Voith-Schneider	2952	204	8.6	37.5
4	Area 1a, T 18 Berths 1, 2; T 30	50	Container / Margrit Rickmers	Docking	Ship's main power	4113	25	26.5	25.2
5	Area 1a, T 18 Berths 1, 2; T 30	50	Container / Margrit Rickmers	Undocking	Bow Thruster	3000	216	9.8	19.3
6	Area 2, Slip 36	40	USCG Ice Breaker Polar Star	Docking	3 Controllable pitch props	2238	200	16	18.2
7	Area 2, Slip 36	40	USCG Cutter Hamilton Class	Docking	2 Controllable Pitch props	1343	200	13	27.2
8	Area 3, Slip 27	30	Tug / Hunter D	Docking a barge	2 Standard props	1276	160	6.2	30.1
9	Area 4, 4a, 4b, 5	40	Tug / Eagle	Docking a barge	Twin ducted props	1119	160	6.4	27.7
10	Area 6	20	Tug / Eagle	Docking a barge	Twin ducted props	1119	160	6.4	7.7
11	Area 7	30	Tug / Eagle	Docking a barge	Twin ducted props	1119	160	6.4	17.7
12	Area 8	20	Tug / Alaska Mariner	Docking	2 Nautican Nozzle	149	50	8.7	5.0
13	Area 1b, 1c Terminals 18, 30	50	Tug / Garth Foss	Assist container ship navigating waterway	Voith-Schneider	1968	140	8.6	37.5
14	Area 4a, South T30 (future)	46	Container / Margrit Rickmers	Docking	Ship's main power	4113	35	26.5	21.2
15	Area 4a, South T30 (future)	46	Container / Margrit Rickmers	Undocking	Bow Thruster	3000	216	9.8	15.3

3. JETWASH Modeling Results

3.1. Scenario 1 Area 1a Terminal 18 Berths 1 and 2

The largest container ships in the waterway call at Berths 1 and 2 and are represented by the Xin Mei Zhou, a 102,453 DWT vessel. This ship has a capacity of 8,530 TEU and is pictured in Figure 4. Propwash generated by the ship's main propulsion is simulated for Scenario 1. The area of propwash modeling is Berths 1 and 2 of Terminal 18, as shown in Figure 5, was assumed for this propwash study. In simulating propwash of the Xin Mei Zhou a minimum underkeel clearance of 4 feet was assumed, corresponding to a draft of 46 feet.

Modeled propwash velocity generated by the ship's main propulsion during docking is shown in Figure 5. The figure shows the horizontal plane of the pattern of near-bottom velocity. The maximum near-bottom velocity is simulated equal to 9.3 ft/sec. The bottom boundary shear stress corresponding to this velocity is 0.32 lbs/ft^2 (15 Pa).

Figure 4. Container ship Xin Mei Zhou (area 1) (photo credit: Tony Finnerty)

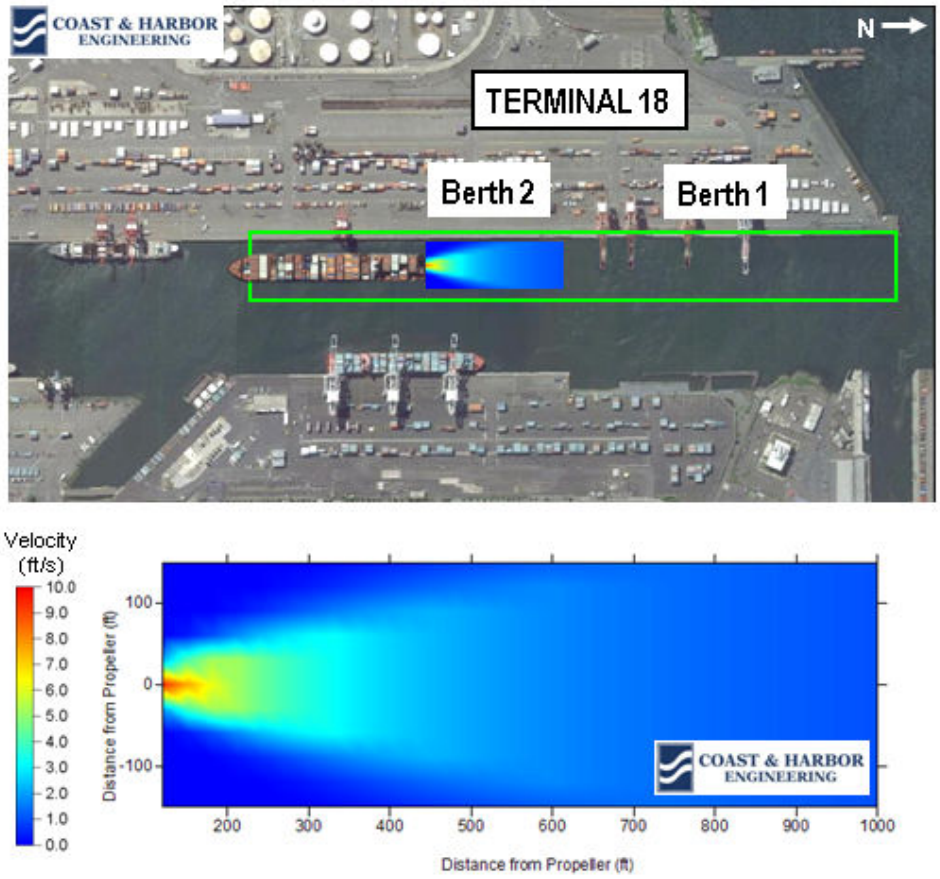

Figure 5. Scenario 1 propwash modeling area and bottom velocity pattern in Area 1a

3.2. Scenario 2 Area 1a Terminal 18 Berths 1 and 2

The vessel Xin Mei Zhou is assumed to undock using the bow thruster initially at full power. All container ships operating in the waterway are assumed to be fitted with a bow thruster and the Xin Mei Zhou represents the most powerful thruster and that located closest to the channel bottom. For conservatively examining propwash generated bottom velocity, the vessel draft upon departing was assumed to be the same as when arriving. A diagram illustrating the size and location of a bow thruster on a container ship is shown in Figure 6. Thruster wash generated by the bow thruster is simulated in Scenario 2. Modeled velocity generated by the ship's thruster during undocking is shown in Figure 7. The figure shows the horizontal plane of the pattern of near-bottom velocity in two zones of intensity. The maximum near-bottom velocity is 11.4 ft/sec. The bottom boundary shear stress corresponding to this velocity is 0.48 lbs/ft^2 (23 Pa). The figure illustrates the concept that as the ship moves farther from the berth the thruster power is reduced, resulting in zone of bottom velocity less than the maximum nearer the channel center.

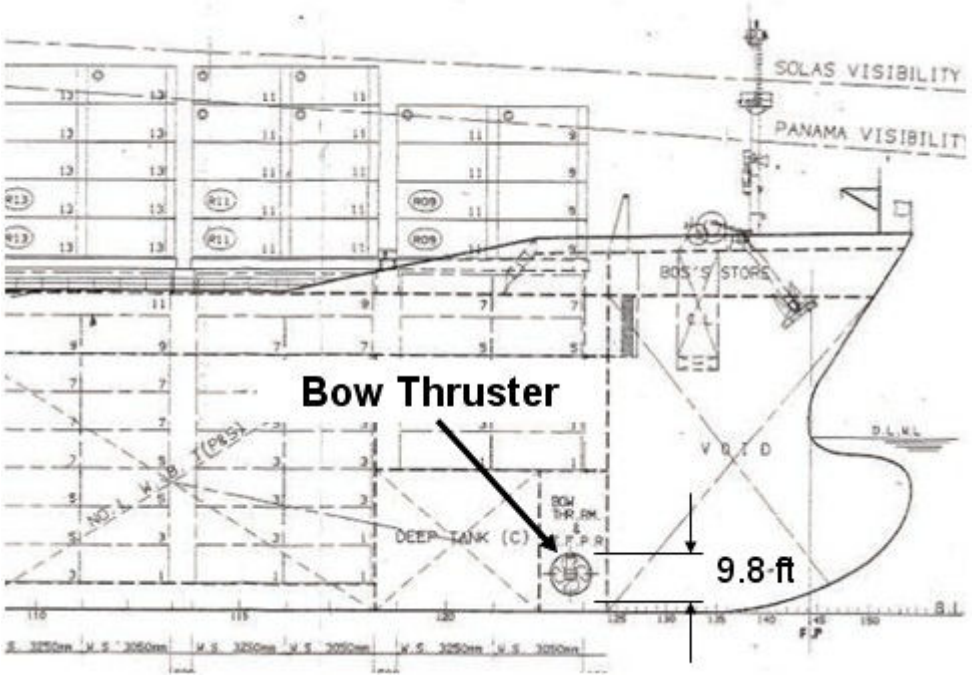

Figure 6. Bow thruster configuration on container ship hull

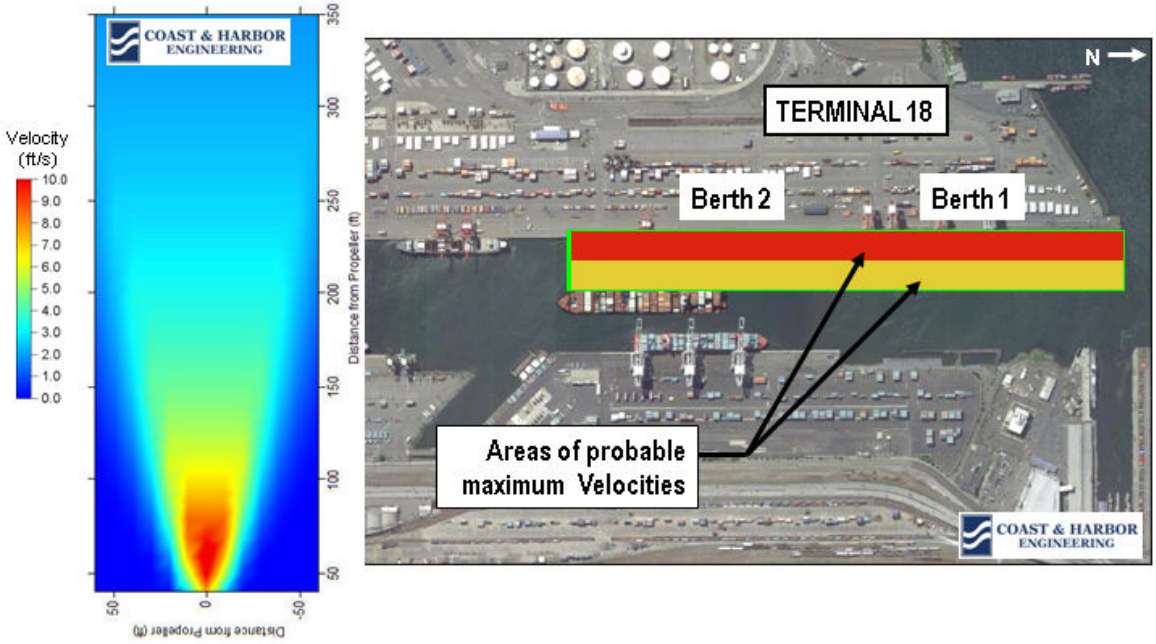

Figure 7. Scenario 2 thruster wash modeling area and bottom velocity pattern in Area 1a

3.3. Scenario 3 Areas 1a, 1b

Tugs assisting container ships during docking, undocking, and navigating in the waterway are represented by the tug Garth Foss shown in Figure 8. The tug is powered by Voith-Schneider Propulsors and can develop 7,600 horsepower. Propwash generated by the two propulsors is simulated in Scenario 3.

Modeled velocity generated by the tug during application of 50 percent power is shown in Figure 9. The figure shows the horizontal plane of the pattern of near-bottom velocity. The maximum near-bottom velocity is 3.6 ft/s. The bottom boundary shear stress corresponding to this velocity is 0.05 lbs/ft^2 (2 Pa).

Figure 8. Tug representative of Garth Foss, assisting container ships (photo credit: Peter Kim)

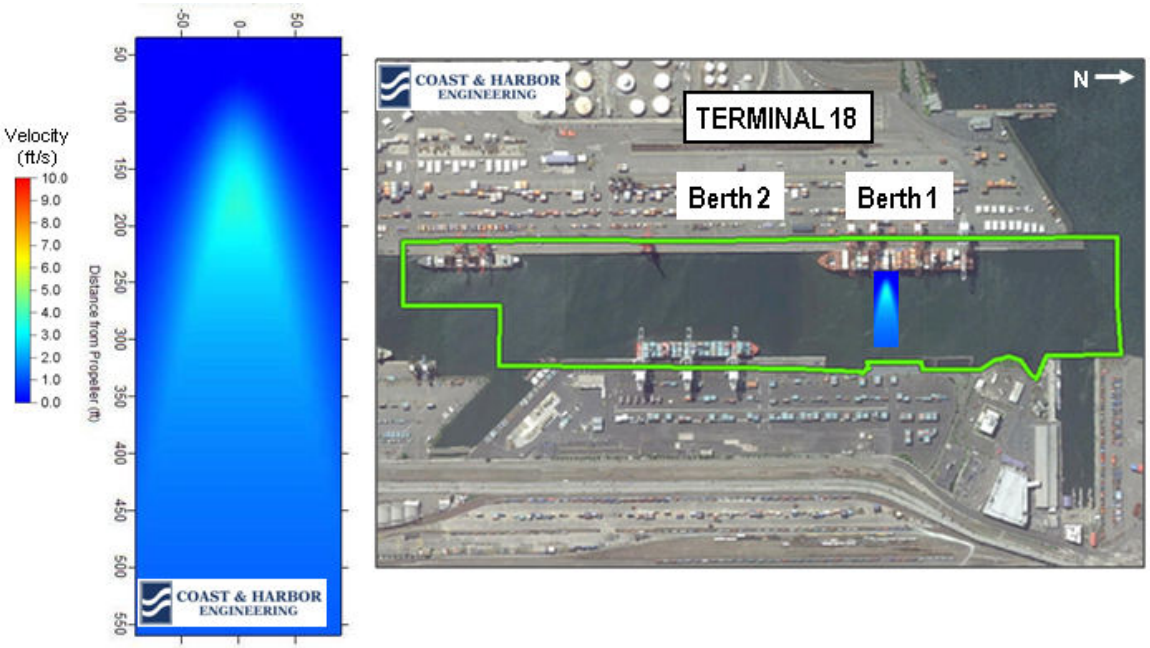

Figure 9. Pattern of near-bottom velocity of tug Garth Foss in Area 1a, 1b

3.4. Scenario 4 Area 1a Terminal 18 Berths 3 and 4, Terminal 30

A container ship representing those calling at Berths 3 and 4 and at Terminal 30 is the Margrit Rickmers, a 67,550 DWT vessel. This ship has a capacity of 5,080 TEU and is pictured in Figure 10. The maximum draft is 39.1 ft. Propwash generated by this ship's main propulsion is simulated for Scenario 4. The area of propwash modeling is Berths 3 and 4 and Terminal 30 in Area 1a, as shown in Figure 11.

Modeled propwash velocity generated by the ship's main propulsion during docking is shown in Figure 11. The figure shows the horizontal plane of the pattern of near-bottom velocity. The maximum near-bottom velocity is 6.3 ft/sec. The bottom boundary shear stress corresponding to this velocity is 0.15 lbs/ft^2 (7 Pa).

Figure 10. Container ship Margrit Rickmers (area 1a)

3.5. Scenario 5 Area 1a Terminal 18 Berths 3 and 4, Terminal 30

The vessel Margrit Rickmers is assumed to undock using the bow thruster at full power. The position and dimensions of the bow thruster are shown in Figure 6. Thruster wash generated by the bow thruster is simulated in Scenario 5. For conservatively examining propwash generated bottom velocity, the vessel draft upon departing was assumed to be the same as when arriving. The area of thrusterwash modeling is Berths 3 and 4 of Terminal 18 and all of Terminal 30 in Area 1a, as shown in Figure 12.

Modeled velocity generated by the ship's thruster during undocking is shown in Figure 12. The figure shows the horizontal plane of the pattern of near-bottom velocity. The maximum near-bottom velocity is 7.1 ft/sec. The bottom boundary shear stress corresponding to this velocity is 0.19 lb/ft^2 (9 Pa).

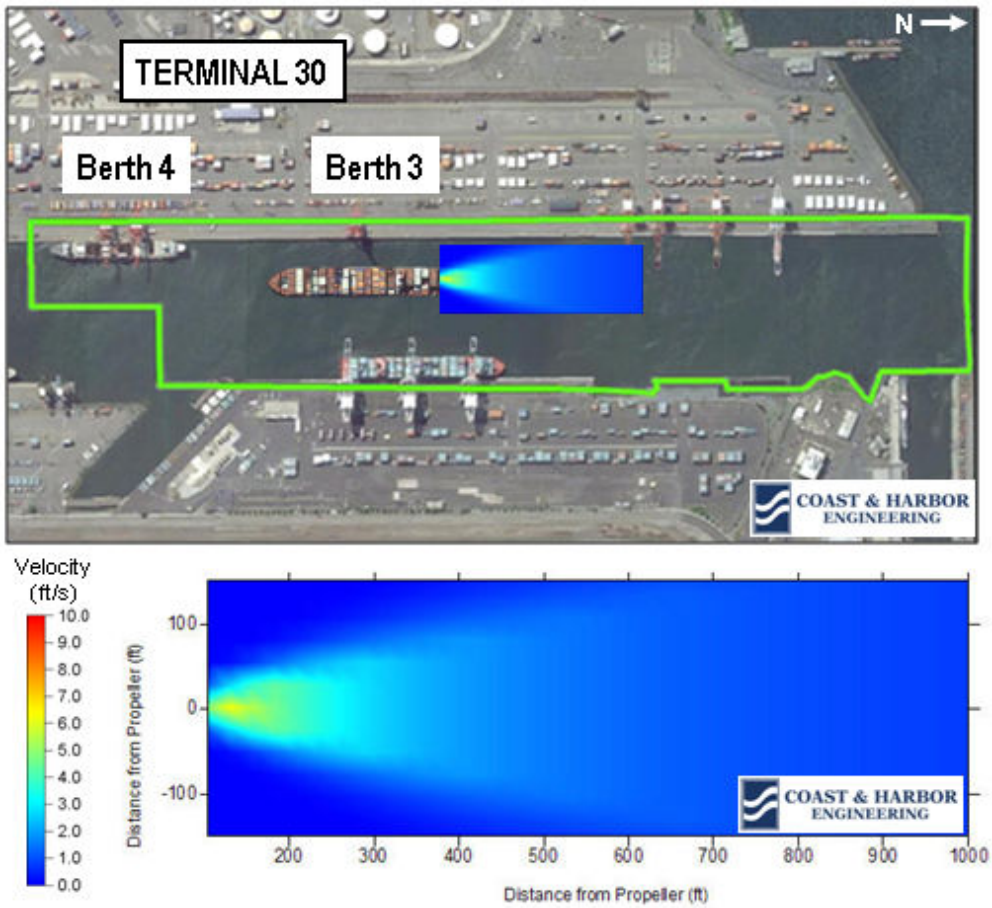

Figure 11. Pattern of near-bottom velocity of Margrit Rickmers main propulsion in Area 1a

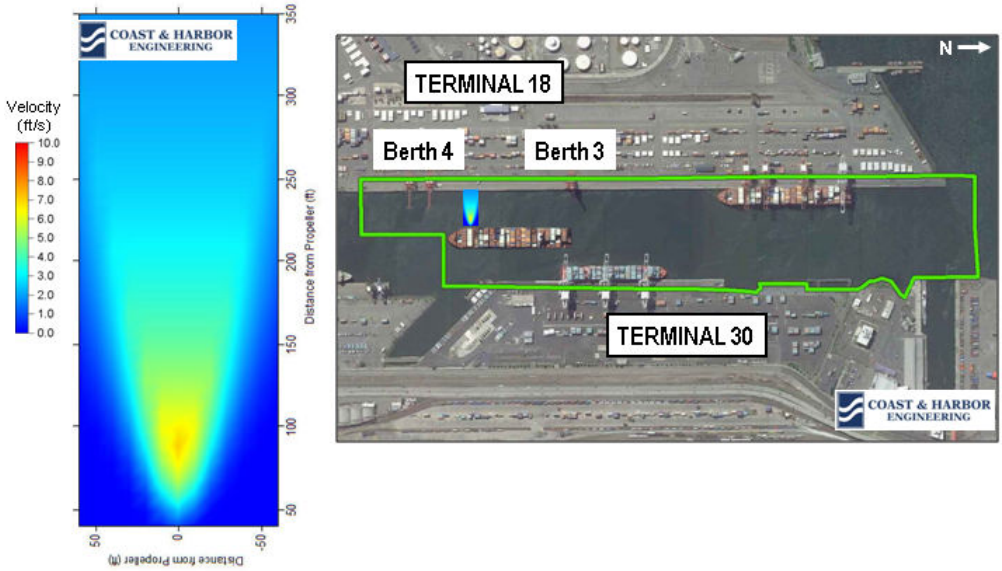

Figure 12. Pattern of near-bottom velocity of Margrit Rickmers bow thruster in Area 1a

3.6. Scenario 6 Area 2 Slip 36

Coast Guard vessels identified as sources of propwash having the potential for initiating bottom sediment movement Area 2 are the Polar class icebreakers and the Hamilton class high endurance cutters. The icebreakers have a loaded draft of 32 ft and have three controllable pitch propellers arranged as shown in a photograph of the Polar Sea, Figure 13. The area of propwash modeling is Slip 36, as shown in Figure 14.

Modeled propwash velocity generated by the main propulsion of the Polar class icebreaker during docking is shown in Figure 14. The figure shows the horizontal plane of the pattern of near-bottom velocity. The maximum near-bottom velocity is 6.5 ft/sec. The bottom boundary shear stress corresponding to this velocity is 0.16 lb/ft^2 (8 Pa).

Figure 13. Polar Sea in dry dock showing propellers and rudder (area 2)

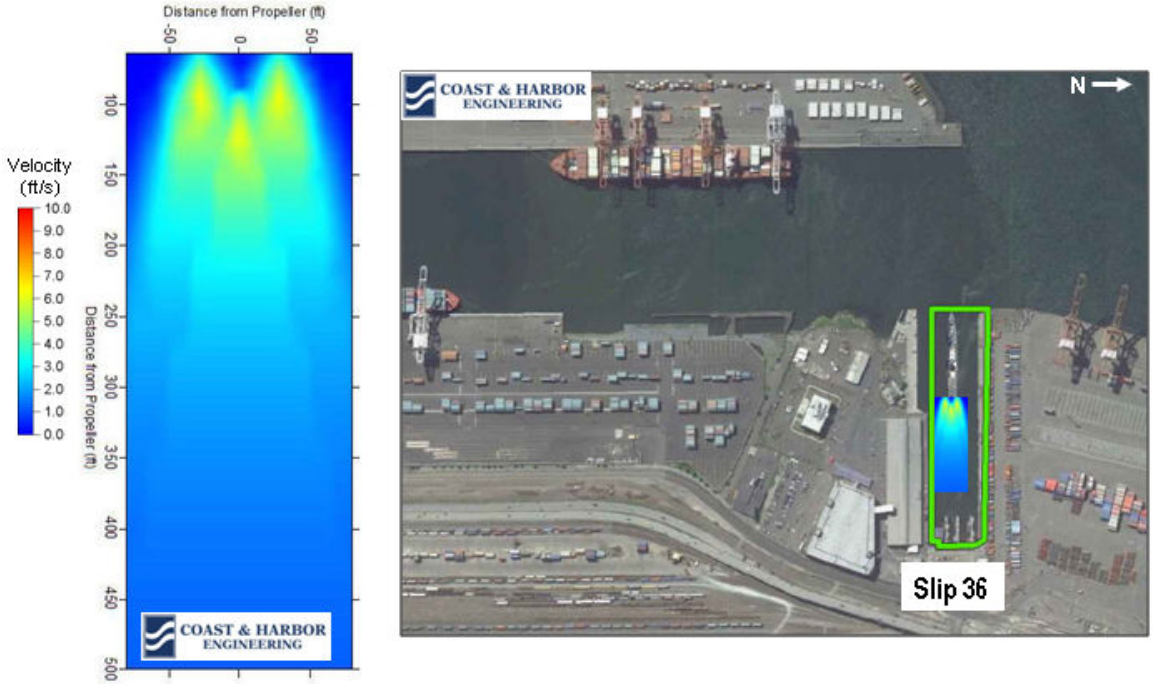

Figure 14. Pattern of near-bottom velocity of Polar class icebreaker propwash in Area 2

3.7. Scenario 7 Area 2 Slip 36

The Hamilton class Coast Guard cutter has a draft of 20 ft and has twin controllable pitch propellers. The cutter was modeled for determining the potential for initiating bottom sediment movement Area 2. The ship profile is shown in Figure 15. These cutters are fitted with retractable thrusters that are capable of outputting 350 horsepower, which was not simulated because the power is small relative to the main propulsion. The area of propwash modeling is Slip 36, as shown in Figure 16.

Modeled propwash velocity generated by the main propulsion of the Hamilton class cutter during docking is shown in Figure 16. The figure shows the horizontal plane of the pattern of near-bottom velocity. The maximum near-bottom velocity is 4.5 ft/sec. The bottom boundary shear stress corresponding to this velocity is 0.08 lbs/ft^2 (4 Pa).

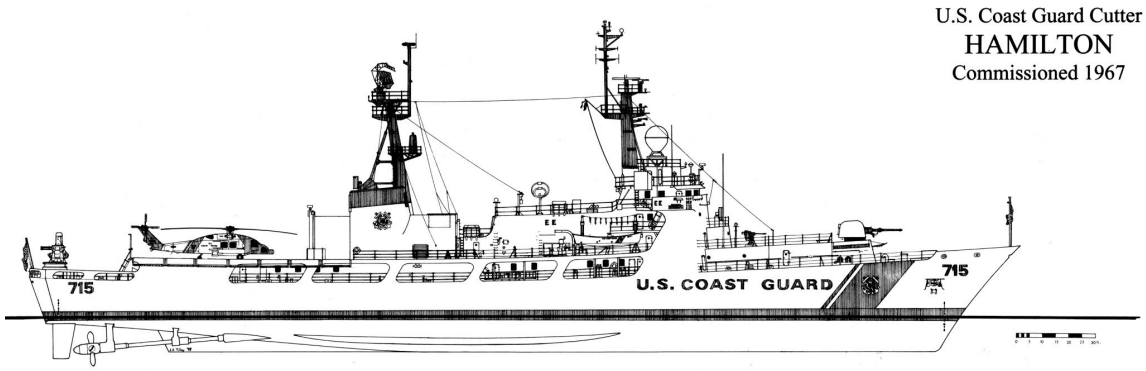

Figure 15. Ship profile of Hamilton class cutter (area 2)

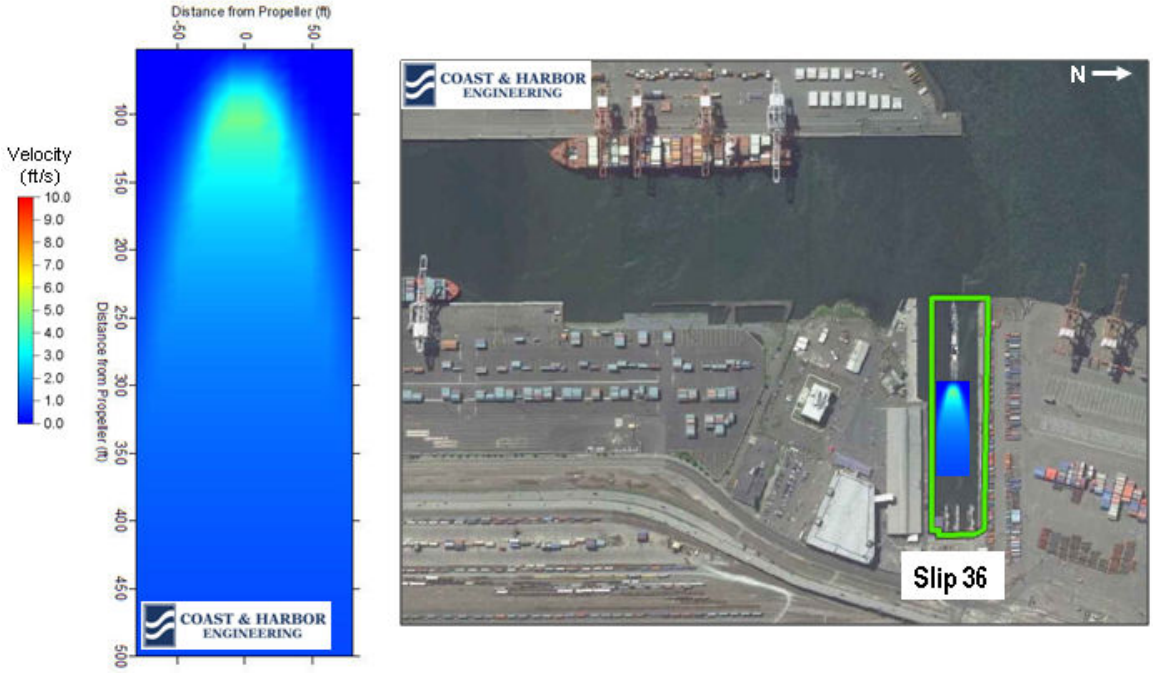

Figure 16. Pattern of near-bottom velocity of Cutter Hamilton propulsion in Area 2

3.8. Scenario 8 Area 3 Slip 27

Vessel activity at Area 3 consists of tugs taking barges to and moving barges from the slip, represented by the tug Hunter D. The tug is pictured in Figure 17. The Hunter D has a draft of 14.1 ft and is powered by two engines that can develop 3,420 horsepower each. The area of propwash modeling is Slip 27, as shown in Figure 18.

Modeled propwash velocity generated by the tug Hunter D during maneuvering is shown in Figure 18. The figure shows the horizontal plane of the pattern of near-bottom velocity. The maximum near-bottom velocity is 3.0 ft/sec. The bottom boundary shear stress corresponding to this velocity is 0.03 lb/ft^2 (2 Pa).

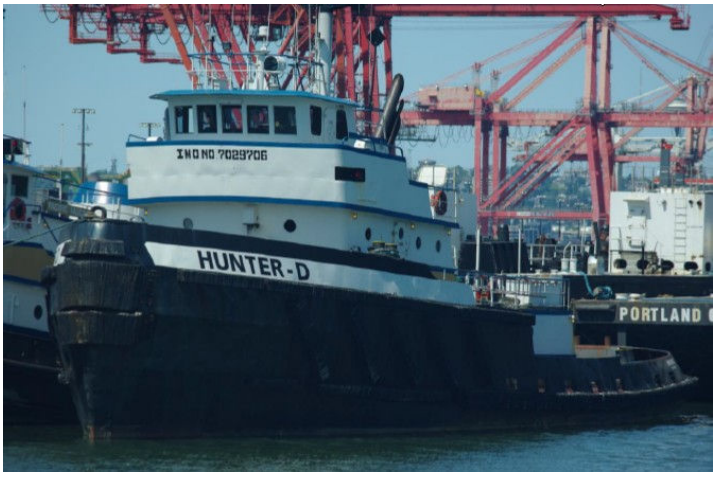

Figure 17. Tug Hunter D (Area 3)

Figure 18. Pattern of near-bottom velocity of Tug Hunter D in Area 3

3.9. Scenario 9 Areas 4, 4a, 4b and 5

The tug Eagle represents tugs that maneuver barges at South Terminal 30 (Area 4 and 4a) and that assist bulk carriers that call at the south end of Terminal 18 (Area 5). Area 4b is assumed to be subjected to similar propwash velocity from vessels maneuvering at adjacent areas. The tug is pictured in Figure 19. The Eagle has a draft of 16.5 ft and is powered by two engines that can develop 3,000 horsepower each. The tug is assumed to apply 75 percent of available power in these areas.

Modeled propwash velocity generated by the tug Eagle during maneuvering in Areas 4, 4a, 4b, and 5 is shown in Figure 20. Bottom elevation in these areas is -40 ft. The figure shows the horizontal plane of the pattern of near-bottom velocity. The maximum near-bottom velocity is 3.0 ft/sec. The bottom boundary shear stress corresponding to this velocity is 0.03 lb/ft2 (2 Pa).

Figure 19. Tug Eagle (Areas 4, 4a, 4b and 5)

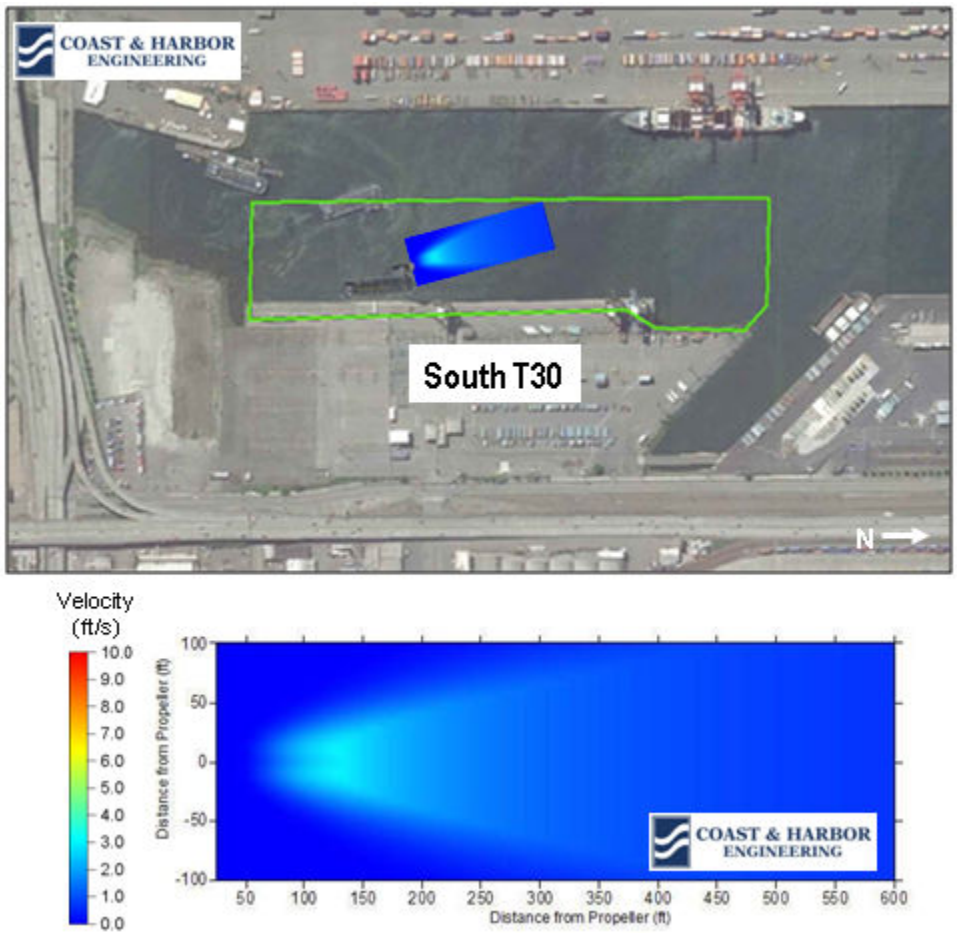

Figure 20. Pattern of near-bottom velocity of tug Eagle in Areas 4, 4a, 4b and 5

3.10. Scenario 10 Area 6

The tug Eagle represents tugs that maneuver at the west side of the waterway north of the West Seattle Bridge (Area 6). The tug is pictured in Figure 19. The Eagle is assumed to apply 50 percent of available power in this area. Area 6 for propwash modeling is shown in Figure 21.

Modeled propwash velocity generated by the Tug Eagle during maneuvering is shown in Figure 21. Bottom elevation in this area is -20 ft. The figure shows the horizontal plane of the pattern of near-bottom velocity. The maximum near-bottom velocity is 10.6 ft/sec. The bottom boundary shear stress corresponding to this velocity is 0.45 lb/ft^2 (22 Pa).

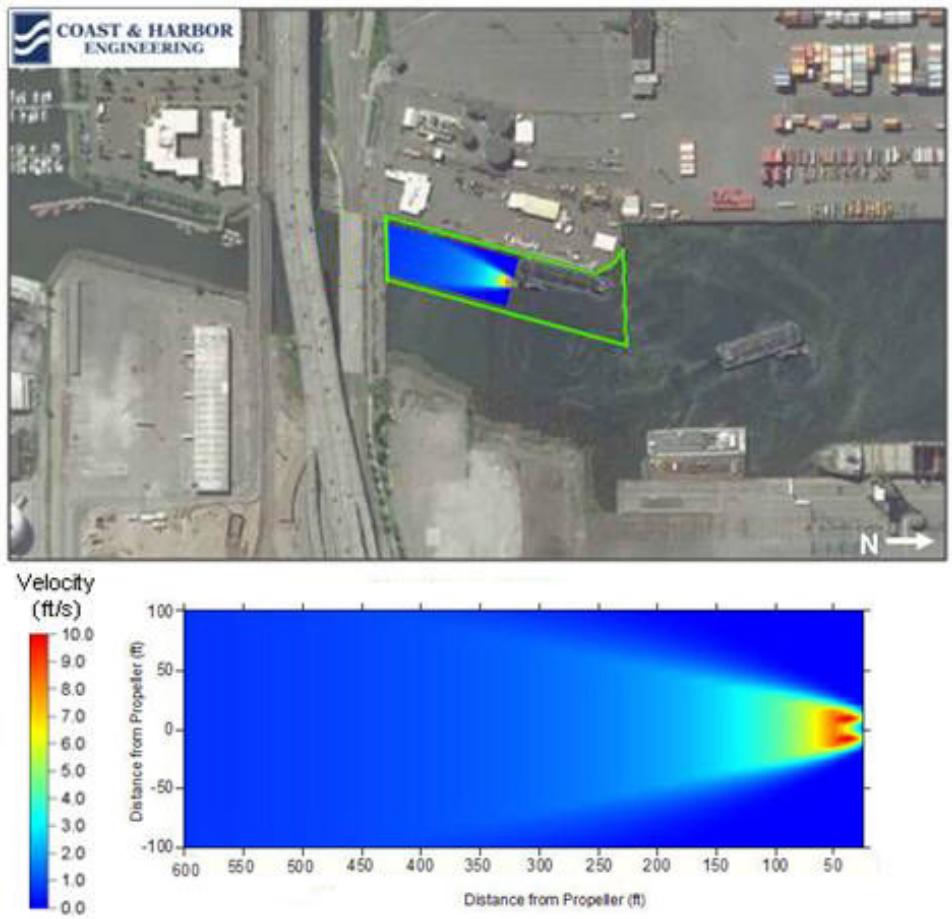

Figure 21. Pattern of near-bottom velocity of Tug Eagle in Area 6

3.11. Scenario 11 Area 7

The tug Eagle represents tugs that transit this eastern part of the waterway north of the bridge (Area 7). The tug is pictured in Figure 19. The Eagle is assumed to apply 50 percent of available power in this area. Area 7 for propwash modeling is shown in Figure 22.

Modeled propwash velocity generated by the tug Eagle during maneuvering is shown in Figure 22. Bottom elevation in this area is -30 ft. The figure shows the horizontal plane of the pattern of near-bottom velocity. The maximum near-bottom velocity is 4.7 ft/sec. The bottom boundary shear stress corresponding to this velocity is 0.08 lb/ft^2 (4 Pa).

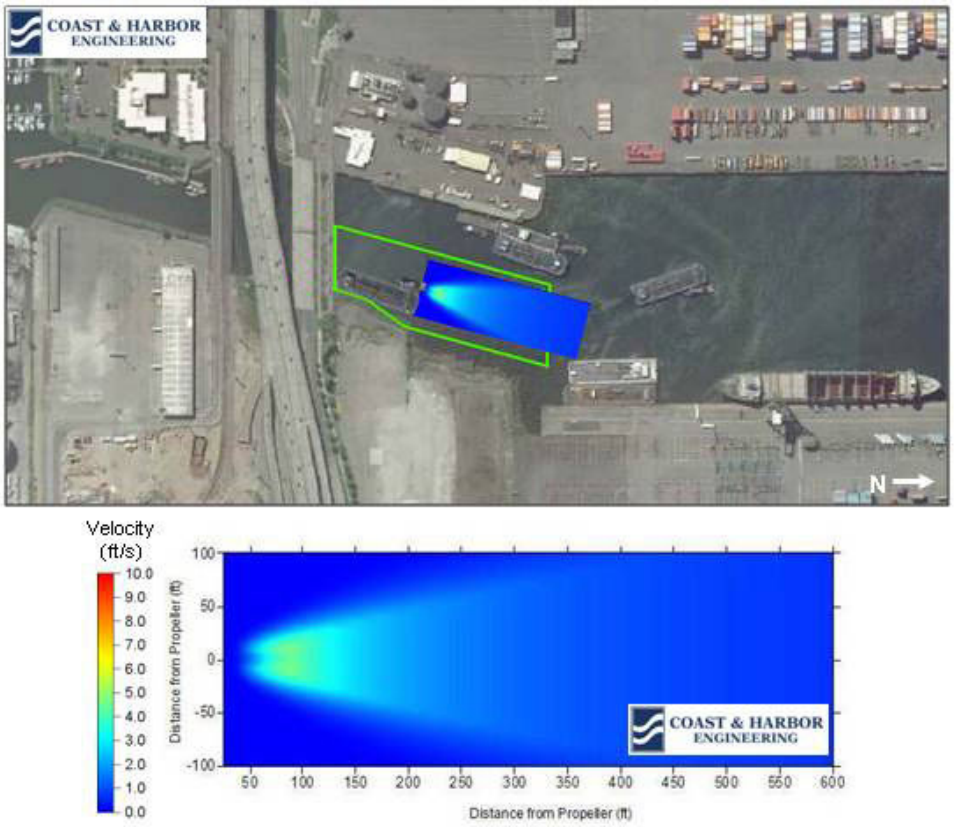

Figure 22. Pattern of near-bottom velocity of Tug Eagle in Area 7

3.12. Scenario 12 Area 8

The tug Alaska Mariner represents the largest of the Western Towboat fleet that moors in Area 8. This tug has a draft of 14.1 ft and is powered by twin engines each developing 2,260 horsepower. The Alaska Mariner is pictured in Figure 23. The area of propwash modeling is shown in Figure 24.

Modeled propwash velocity generated by the tug Alaska Mariner during maneuvering in Area 8 is shown in Figure 24. Bottom elevation in this area is -20 ft. The figure shows the horizontal plane of the pattern of near-bottom velocity. The maximum near-bottom velocity is 4.2 ft/sec. The bottom boundary shear stress corresponding to this velocity is 0.07 lb/ft^2 (3 Pa).

Figure 23. Tug Alaska Mariner (area 8)

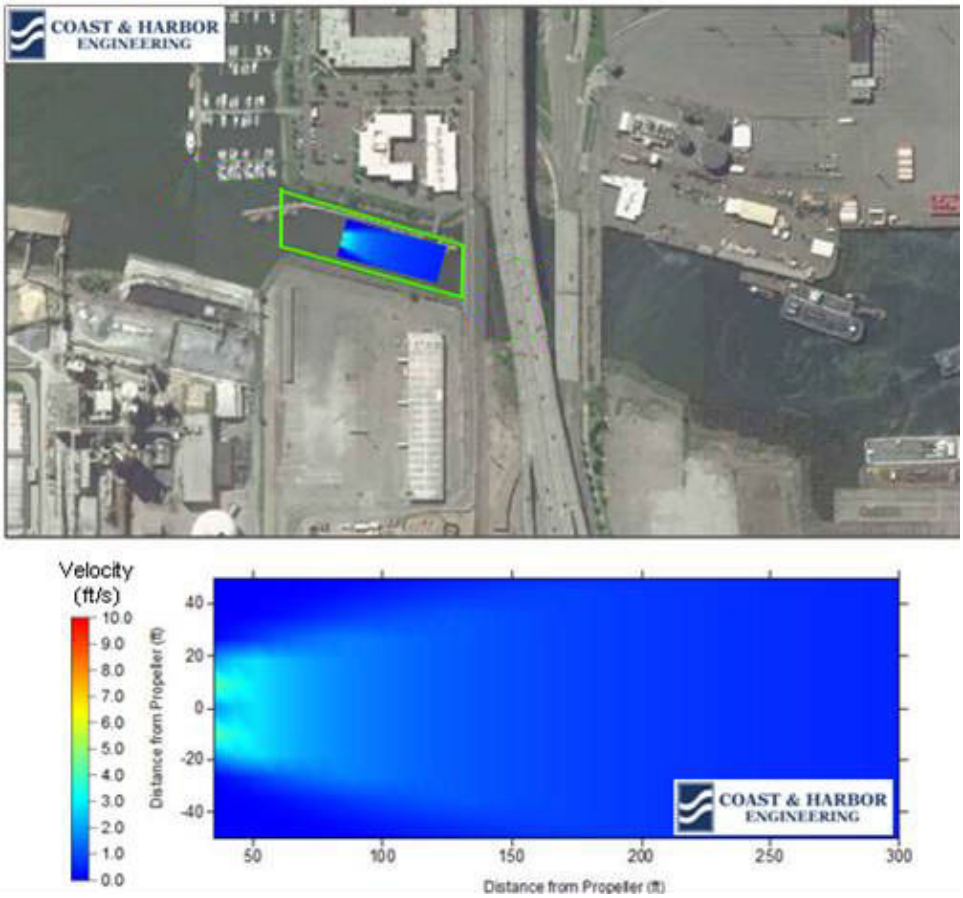

Figure 24. Pattern of near-bottom velocity of Tug Alaska Mariner in Area 8

3.13. Scenario 13 Navigating in East Waterway

Container ships are moved into East Waterway bow first by at least two tugs when mooring at Terminal 18. Tugs are at the bow and stern, and the ship's thruster aids in steering the ship in the waterway. Container ships mooring at Terminal 30 enter the waterway stern-first, under the assistance of at least two tugs. The tug Garth Foss (see Figure 8) represents tugs that assist ships in the East Waterway. Tug speed is assumed to be 4 knots and the maximum power applied while moving a ship into or out of the waterway is assumed to be 50 percent of available power.

Modeled propwash velocity generated by the tug Garth Foss during assisting in Area 1b using the steady-state JETWASH model is shown in Figure 25. Bottom elevation in this area is -50 ft. The figure shows the horizontal plane of the pattern of near-bottom velocity. The maximum near-bottom velocity computed with JETWASH is 3.0 ft/sec. The bottom boundary shear stress corresponding to this velocity is 0.03 lbs/ft^2 (2 Pa). These values are considered to be conservative. Fully accounting for vessel speed will reduce these values of velocity and stress. Because of the limitation of the JETWASH model in simulating effects of moving vessels, and the availability of the unsteady model VH-PU to simulate this condition, the next phase of the study will employ VH-PU. Values calculated with the tool that incorporates vessel movement are expected to be less than that illustrated in Figure 25.

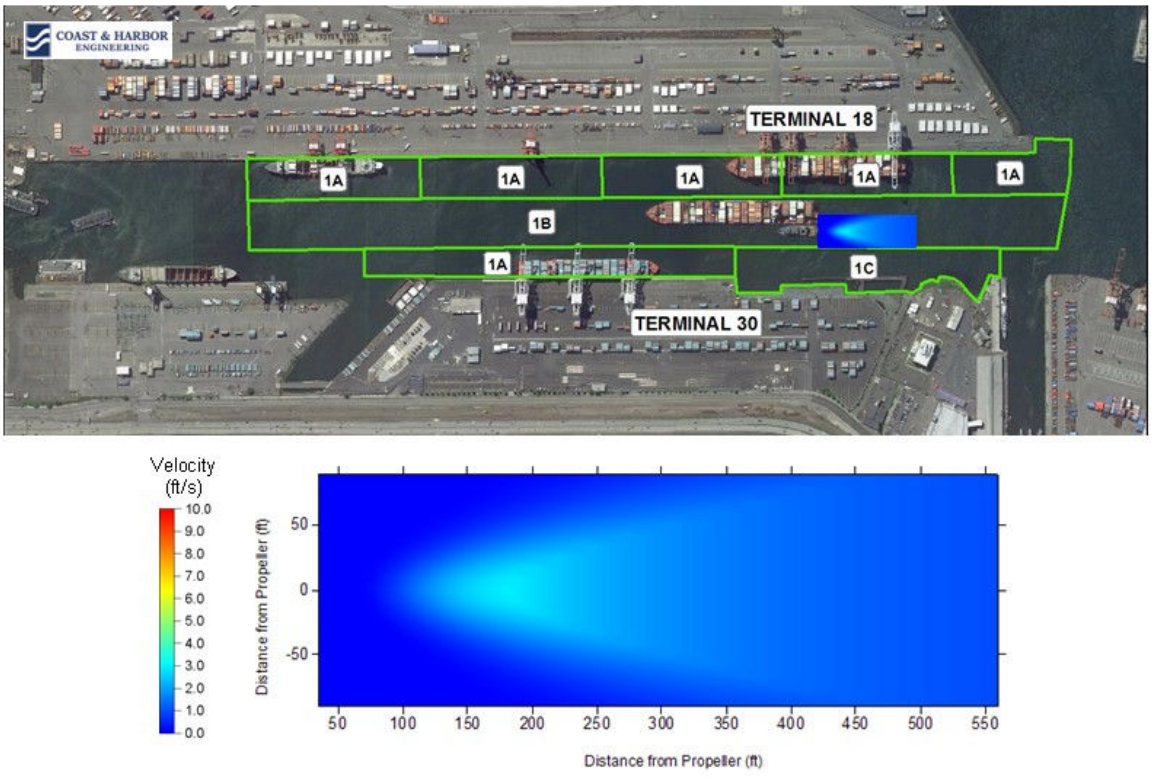

Figure 25. Pattern of near-bottom velocity of Tug Garth Foss while assisting a ship in Area 1b

3.14. Scenario 14 Area 4a

Scenario 14 is developed to represent future conditions at South Terminal 30. It is assumed that berthing area at the terminal will be dredged to -46 ft MLLW to accommodate a container ship Margrit Rickmers, a 67,550 DWT of 5,080 TEU capacity vessel (see Figure 10). The maximum draft of the ship of this scenario is assumed at 39.1 ft.

Modeled propwash velocity generated by the ship's main propulsion during docking is shown in Figure 26. The figure shows the horizontal plane of the pattern of near-bottom velocity. The maximum near-bottom velocity is 7.0 ft/sec. The bottom boundary shear stress corresponding to this velocity is 0.18 lbs/ft^2 (9 Pa).

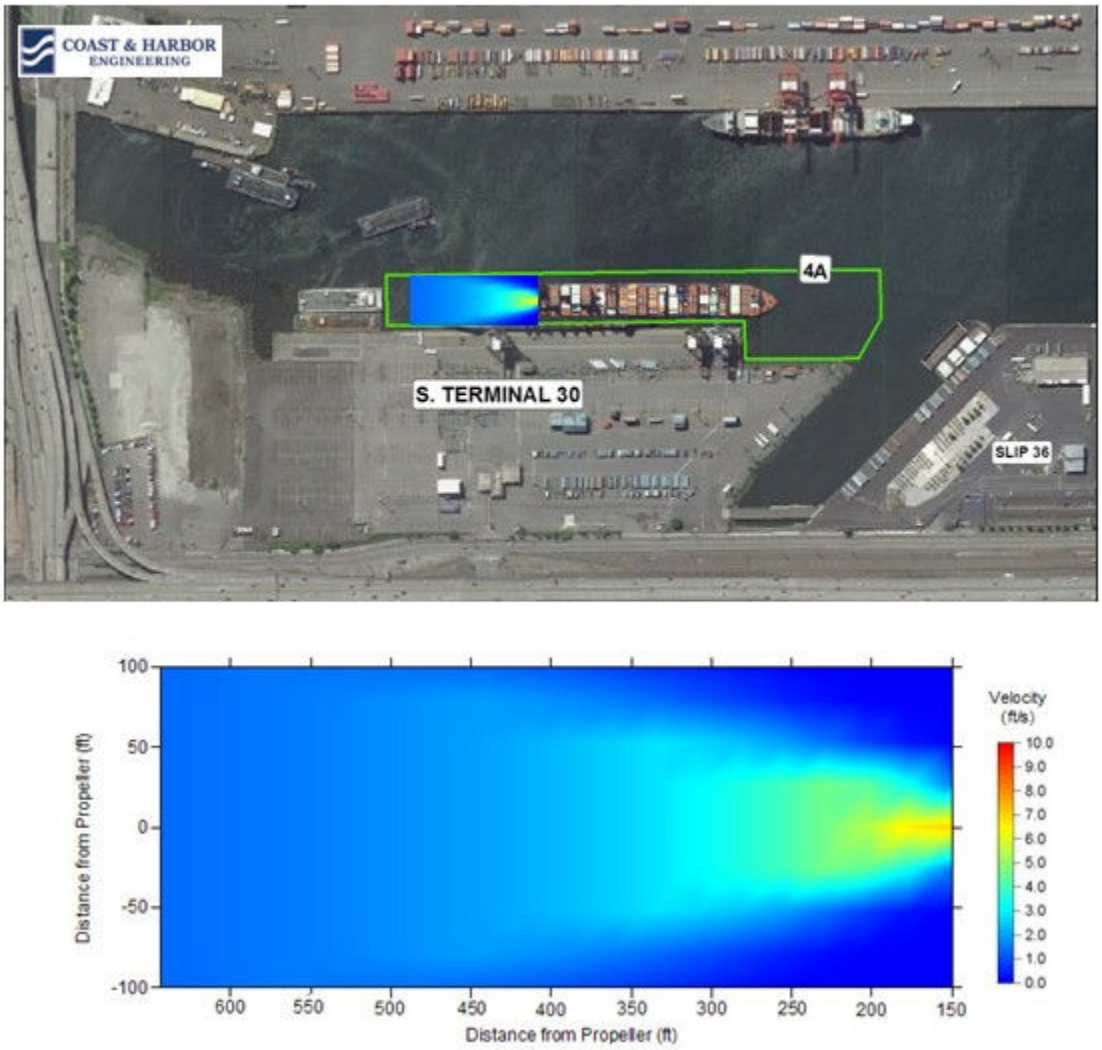

Figure 26. Pattern of near-bottom velocity of Margrit Rickmers main propulsion in Area 4, docking

3.15. Scenario 15 Area 4a, South Terminal 30

Scenario 15, similar to Scenario 14 was developed to represent future conditions at South Terminal 30. Similar to the other scenario a berthing area at the terminal is dredged in the model to -46 ft MLLW to accommodate a container ship Margrit Rickmers.

The vessel Margrit Rickmers is assumed to undock using the bow thruster at full power. The position and dimensions of the bow thruster are shown in Figure 27. For conservatively examining propwash generated bottom velocity, the vessel draft upon departing was assumed to be the same as when arriving.

Modeled velocity generated by the ship's thruster during undocking is shown in Figure 27. The figure shows the horizontal plane of the pattern of near-bottom velocity. The maximum near-bottom velocity is 9.0 ft/sec. The bottom boundary shear stress corresponding to this velocity is 0.30 lbs/ft^2 (14 Pa).

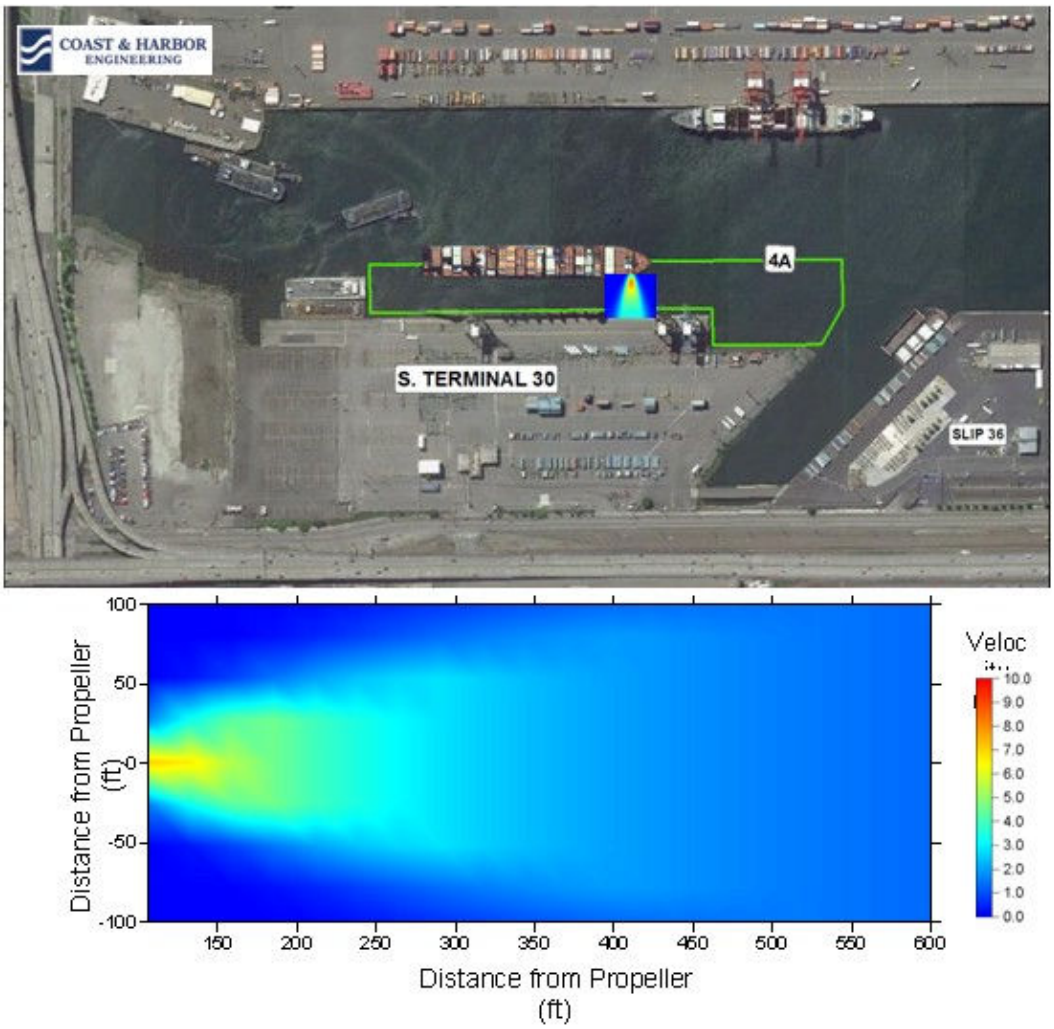

Figure 27. Pattern of near-bottom velocity of Margrit Rickmers bow thrusters in Area 4a, undocking

3.16. Propwash Modeling Summary Results

Simulated maximum near-bottom velocities of these 15 scenarios are shown in the respective analysis areas in Figure 28. As noted in Section 3.13, the listed velocity and shear stress values are conservative and will refined in a future study phase using an unsteady model that better simulates the effect of vessel movement. As noted in Sections 3.14 and 3.15, future conditions of ship berthing in Area 4a were simulated. Figure 28 lists velocities for current conditions, with notes referring to velocities for future conditions. The listed velocity magnitudes apply to each entire analysis area because it is not known where the vessel can be positioned within the area. Figures 29 and 30 summarize the bottom shear stress in units of pounds per square foot and Pascals, respectively, corresponding to the propwash-induced velocities.

Area 1b was designated as the central part of the Waterway where ships navigate to or from the berths. Bottom velocities modeled for Area 1b, presented in Section 3.13 are lower than in adjacent areas. The boundary between Area 1b and Area 1a, however, is not clearly defined. It is possible, and is conservatively assumed, that vessel maneuvers simulated for Area 1a extend into Area 1b and the greater velocities of the two apply to Area 1b. Therefore, the part of Area 1b adjacent to Terminal 18 berths 1 and 2 should be assumed to experience bottom velocity up to 11.4 ft/sec and corresponding bottom shear stress of 0.48 lbs/sq ft (23 Pa). Similarly, bottom velocity up to 7.1 ft/sec may affect the part of Area 1b adjacent to berths 3 and 4, with corresponding bottom shear stress of 0.19 lb/sq ft (9 Pa).

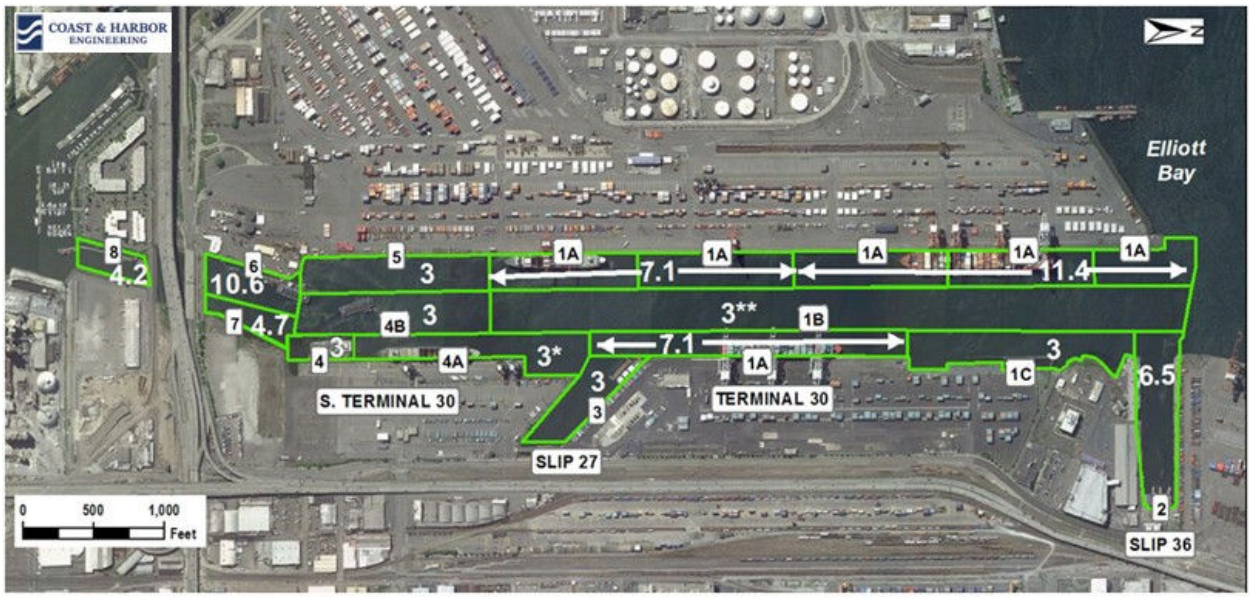

Note: *Future case of Area 4a = 9.0 ft/sec
** Bottom velocity from moving vessel to be refined in unsteady analysis in future phase of study

Figure 28. Summary of near-bottom velocities, all scenarios

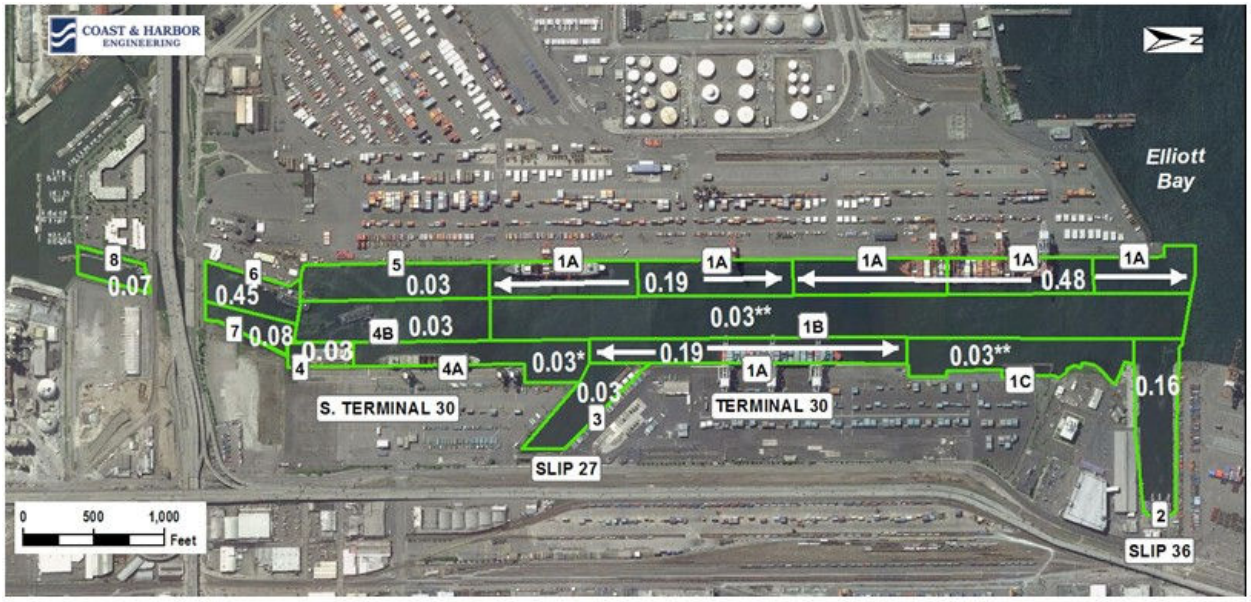

Note: *Future case of Area 4a = 0.30 lbs/sq ft
** Bottom shear stress from moving vessel to be refined in unsteady analysis in future phase of study

Figure 29. Summary of bottom shear stresses (lbs/sq ft), all scenarios

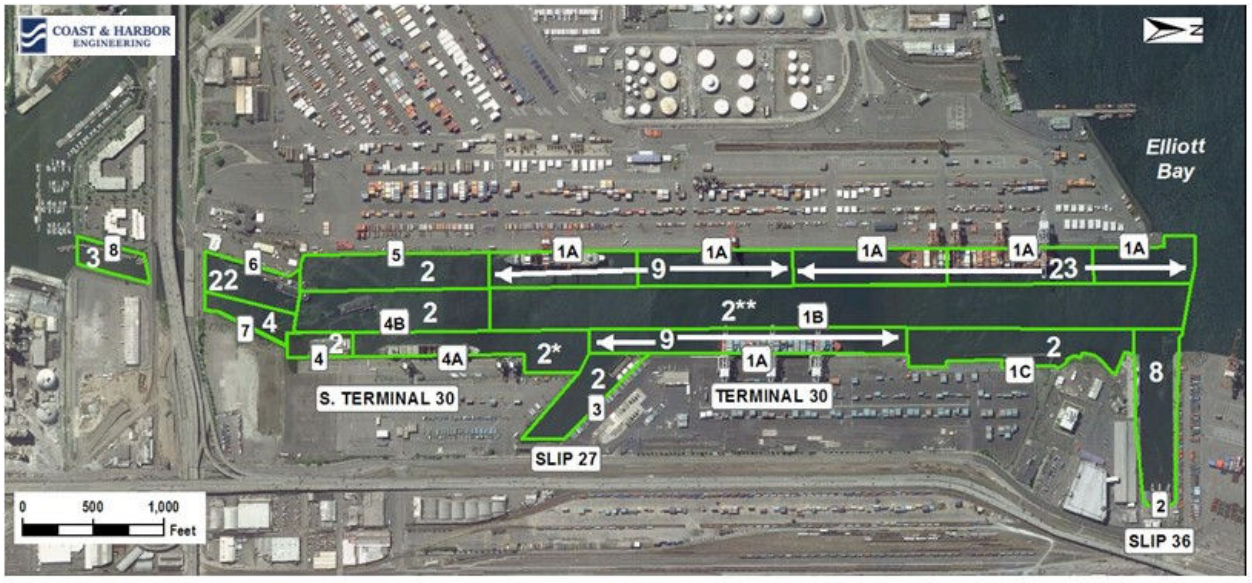

Note: *Future case of Area 4a = 14 Pa
** Bottom shear stress for moving vessel to be refined in unsteady analysis in future phase of study

Figure 30. Summary of bottom shear stresses (Pascals), all scenarios

4. Pressure Field Modeling

Water velocity generated beneath a moving vessel might be an agent for mobilizing sediment on the channel bottom surface if the velocity has sufficient magnitude. Bottom velocity generated by a ship being assisted by a tug along the waterway is investigated in this section. Vessel pressure field hydrodynamic forces were calculated using the Vessel Hydrodynamics Longwave Unsteady (VH-LU) model (Shepsis 2001). The VH-LU model predicts water level and velocity fluctuations surrounding a moving ship and the resulting velocity beneath the hull. The main factors that determine the magnitude of the pressure wave generated by the moving form are the ship's length, beam, draft, shape, and speed at which it moves relative to the water, among other factors.

A container ship representative of those calling at Berths 3 and 4 of Terminal 18 and the assisting tug are vessels selected for pressure field analysis. Analysis results include bottom velocity at a point as the vessel passes above. Channel depth and dimensions are nearly uniform along the length of East Waterway. Therefore, the vessel induced bottom velocity at one location along the sailing line is similar to that at other locations and a single snapshot of velocity pattern is sufficient to characterize conditions in the waterway. Figure 31 shows the bathymetry within the hydrodynamic modeling domain and vessel route. Vessel speed while moving in the waterway is assumed to be 4 knots or less.

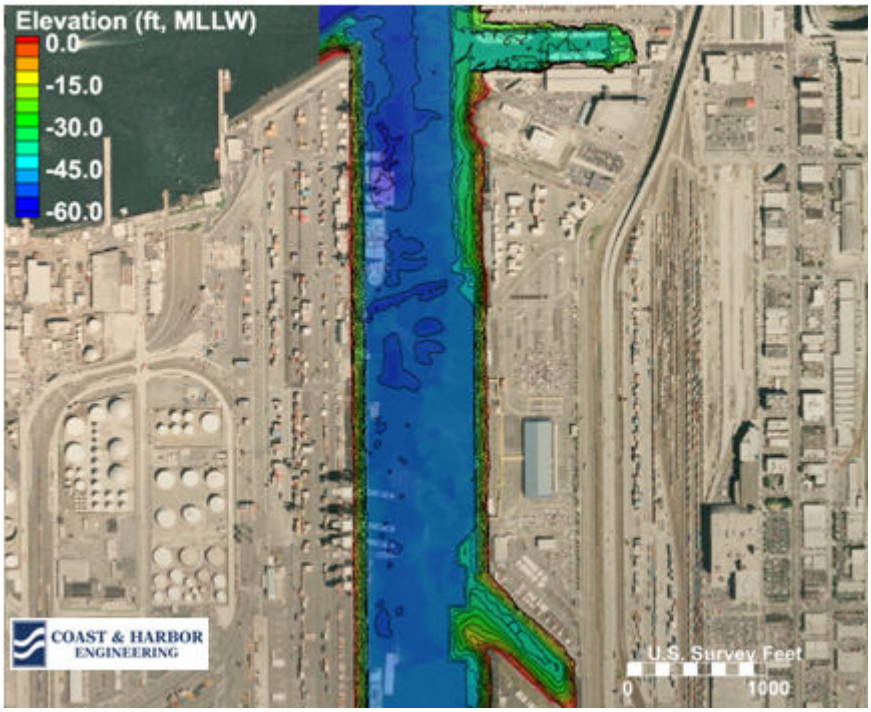

Figure 31. Bathymetry of East Waterway

Figure 32 shows velocity output at a single location of pressure field modeling of a container ship moving inbound along the channel centerline at 4 knots. For this container ship simulation, the maximum water velocity relative to the stationary bed was 1.3 ft/sec, averaged in the 12.9-ft vertical distance between the hull and the bottom. The bottom boundary shear stress corresponding to this velocity is 0.0063 lb/ft^2 (0.30 Pa).

Figure 33 shows the velocity output similarly derived for a tug that would assist the ship in the East Waterway. The assumed tug characteristics are those listed in Table 1. For this tug simulation, the maximum water velocity relative to the stationary bed was less than 1.3 ft/sec, averaged in the 35.5-ft vertical distance between the tug hull and the bottom. The bottom boundary shear stress corresponding to this velocity is 0.0063 lb/ft^2 (0.30 Pa).

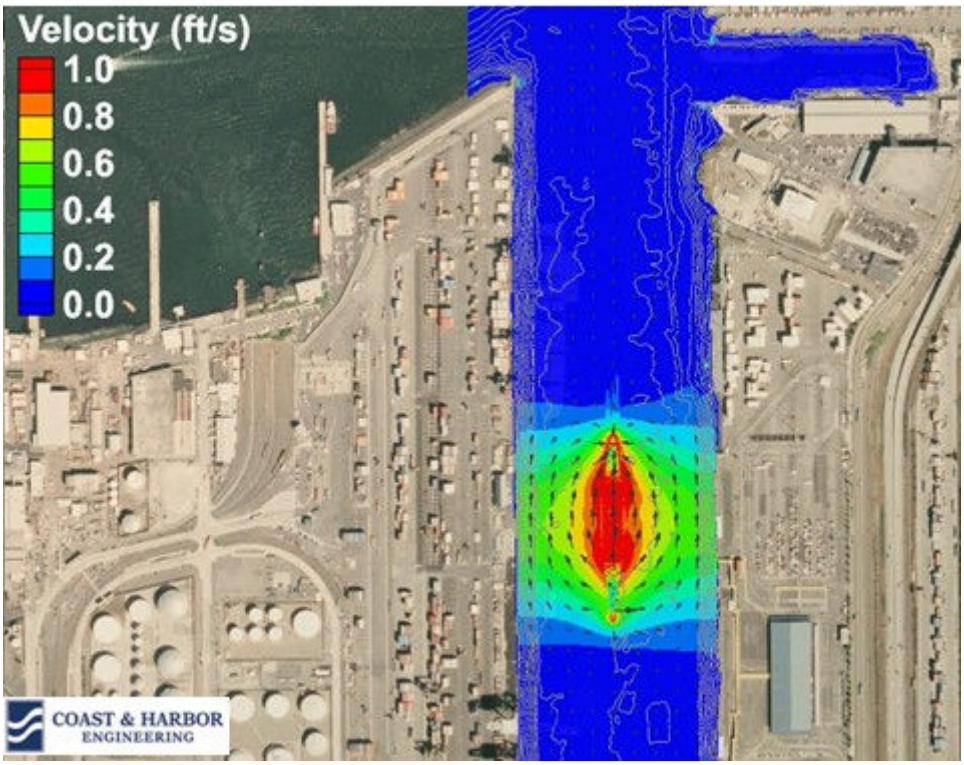

Figure 32. Bottom velocity generated by Margrit Rickmers at 4-knot speed

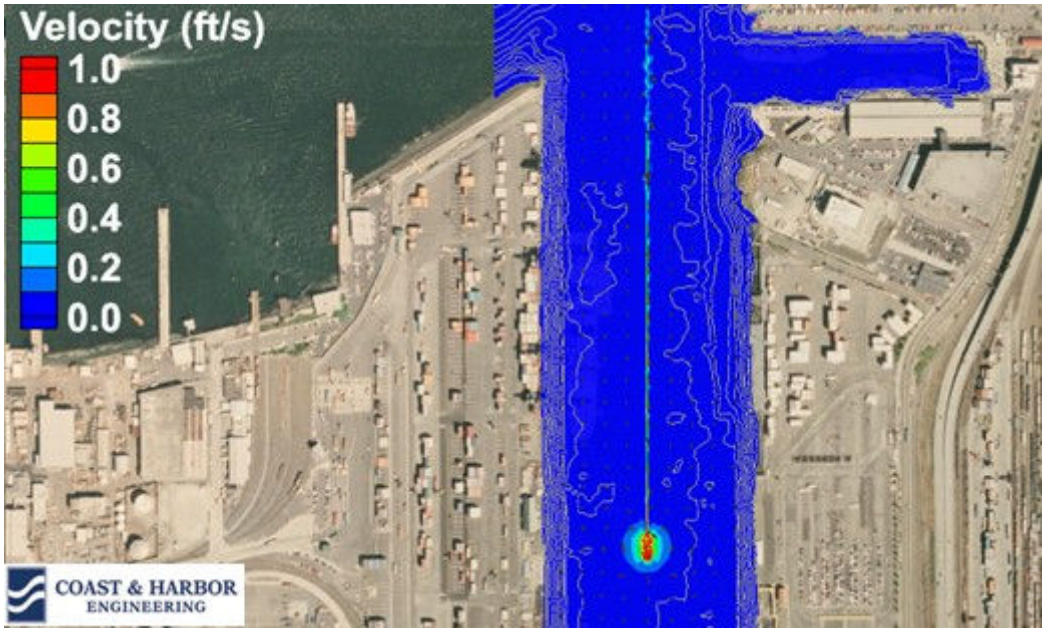

Figure 33. Bottom velocity generated by Garth Foss at 4-knot speed

5. References

Anchor. 2008. Final Sediment Transport Evaluation Approach Memorandum. Memorandum submitted to the U. S. Environmental Protection Agency. Submitted by Anchor Environmental, December 2008.

Blumberg, A.F. and Mellor, G.L. 1987. A description of a three-dimensional coastal ocean circulation model. Three-Dimensional Coastal Ocean Models, N. Heaps (ed), Am. Geoph. Union.

CHE. 2011. Propwash Modeling Scenarios for East Waterway Operable Unit SRI/FS. Technical Memorandum prepared by CHE, March 2011.

CHE. 2003. *Propeller Wash Measurements and Model Comparison - Maury Island Barge Loading Dock*. Technical Memorandum prepared for Northwest Aggregates, August 14, 2003.

Gailani, Joseph, Tahirih Lackey, and S. Jarrell Smith. 2007. "Application of the Particle Tracking Model to predict far-field fate of sediment suspended by nearshore dredging and placement at Brunswick, Georgia." *Proceedings XVIII World Dredging Congress 2007*, WEDA, Lake Buena Vista, Florida, USA.

Shepsis, V. 2001. "Deep-Draft Vessels in Narrow Waterway – Port of Oakland 50-foot Deepening Project." *Proceedings*, Ports 2001 Conference. American Society of Civil Engineers.

U.S. Army Corps of Engineers (USACE). 2002. *Coastal Engineering Manual*. Engineering Manual 1110-2-1100, U.S. Army Corps of Engineers, Washington, D.C. (in 6 volumes).

Vanoni, V. A. 2006. *Sedimentation Engineering*. ASCE Manuals and Reports on Engineering Practice No. 54. American Society of Civil Engineers, Reston, VA. 418 pages.